
MANIPULATING SGD WITH DATA ORDERING ATTACKS

A PREPRINT

Ilya Shumailov
University of Cambridge

Zakhar Shumaylov
University of Cambridge

Dmitry Kazhdan
University of Cambridge

Yiren Zhao
University of Cambridge

Nicolas Papernot
University of Toronto & Vector Institute

Murat A. Erdogdu
University of Toronto & Vector Institute

Ross Anderson
University of Cambridge & University of Edinburgh

April 21, 2021

ABSTRACT

Machine learning is vulnerable to a wide variety of different attacks. It is now well understood that by changing the underlying data distribution, an adversary can poison the model trained with it or introduce backdoors. In this paper we present a novel class of training-time attacks that require no changes to the underlying model dataset or architecture, but instead only change the order in which data are supplied to the model. In particular, an attacker can disrupt the *integrity* and *availability* of a model by simply reordering training batches, with no knowledge about either the model or the dataset. Indeed, the attacks presented here are not specific to the model or dataset, but rather target the stochastic nature of modern learning procedures. We extensively evaluate our attacks to find that the adversary can disrupt model training and even introduce backdoors.

For *integrity* we find that the attacker can either stop the model from learning, or poison it to learn behaviours specified by the attacker. For *availability* we find that a single adversarially-ordered epoch can be enough to slow down model learning, or even to reset all of the learning progress. Such attacks have a long-term impact in that they decrease model performance hundreds of epochs after the attack took place. Reordering is a very powerful adversarial paradigm in that it removes the assumption that an adversary must inject adversarial data points or perturbations to perform training-time attacks. It reminds us that stochastic gradient descent relies on the assumption that data are sampled at random. If this randomness is compromised, then all bets are off.

1 Introduction

The data-driven nature of modern machine learning (ML) training routines puts pressure on data supply pipelines, which become increasingly more complex. It is common to find separate disks or whole content distribution networks dedicated to servicing massive datasets. Multiple workers with different responsibilities are operating on data to provide consistently good performance over the whole training process. This emergent complexity gives a perfect opportunity for an attacker to disrupt ML training, while remaining covert. In the case of stochastic gradient descent (SGD), it assumes uniform random sampling of items from the training dataset, yet in practice this randomness is rarely tested or enforced. Here, we focus on adversarial data sampling.

It is now well known that malicious actors can poison data and introduce backdoors, forcing ML models to behave differently in the presence of triggers [15]. While such attacks have been shown to pose a real threat, they require that the attacker can introduce perturbations or triggers into the dataset used for training.

We show that by simply changing the order in which batches or data points are supplied to a model during training, an attacker can affect model behaviour. More precisely, in this paper we show that it is possible to perform *integrity* and

availability attacks without adding or modifying any data points. For *integrity*, an attacker can reduce model accuracy or arbitrarily control its predictions in the presence of particular triggers. For *availability*, an attacker can increase the amount of time it takes for the model to train, or reset the learning progress.

We present three different types of attacks that exploit *Batch Reordering*, *Reshuffling* and *Replacing* – naming them BRRR attacks. We show that an attacker can significantly change model performance by (i) changing the order in which batches are supplied to models during training; (ii) changing the order in which individual data points are supplied to models during training; and (iii) replacing datapoints from batches with other points from the dataset to promote specific data biases. Furthermore, we introduce Batch-Order Poison (BOP) and Batch-Order Backdoor (BOB), the first techniques that enable poisoning and backdooring of neural networks using only clean data and clean labels; an attacker can control the parameter update of a model by appropriately choosing benign datapoints.

Importantly, BRRR attacks require no underlying model access or knowledge of the dataset. Instead, they focus on the stochasticity of gradient descent, disrupting how well individual batches approximate the true distribution that a model is trying to learn. Another way of looking at them is that they flush out an unexamined assumption behind the stochastic gradient descent technique. As we discuss in Section 4.3, ‘stochastic’ means random; and there are many previous examples of systems which can fail spectacularly if their source of randomness can be undermined somehow by an adversary.

To summarise, we make the following contributions in this paper:

- We present a novel class of attacks on ML models that target the data batching procedure used during training, affecting their integrity and availability. We present a theoretical analysis explaining how and why these attacks work, showing that they target fundamental assumptions of stochastic learning, and are therefore model and dataset agnostic.
- We evaluate these attacks on a set of common computer vision benchmarks, using a range of different hyperparameter configurations, and find that an attacker can slow the progress of training, as well as reset it, with just a single epoch of intervention. Furthermore, even simple manipulations end up having an impact on final model performance.
- We show that data order can poison models and introduce backdoors, even in a blackbox setup. For a whitebox setup, we find that the adversary can introduce backdoors almost as well as if they used perturbed data. While a baseline that uses perturbed data gets 99% trigger accuracy, the whitebox BOB attacker gets $91\% \pm 13$ and the blackbox BOB attacker achieves $68\% \pm 19$.

2 Methodology

2.1 Motivation

ML has revolutionised modern data-processing pipelines by solving extremely sophisticated tasks with little supervision. Originally these models could be trained by anyone, but modern ML has become very power-hungry and now requires specialized hardware [24]. It is common to have models training for extended periods of time, optimizing over neural architectures and parameters [28, 11]. The costs can run to millions of dollars; the models can require enormous datasets and can take whole datacenters to train [7].

Content distribution is usually assumed to be a software engineering question and is rarely handled by ML scientists, making the data pipeline invisible to them. This in turn means that ML engineers will struggle to debug any model problems stemming from data ordering, unless they are as obvious as receiving batches of data with extremely skewed labels¹. We explore whether an attacker who has acquired control over the data sampling procedure can affect model integrity and availability.

Such an attack could be very hard to detect, as it does not change anything about the pipeline; the dataset is still the same and has no perturbations added to it. We assume the strongest possible threat model, where the adversary has no knowledge of the underlying dataset or the underlying model. The blackbox nature of the threat is realistic but, as we shall see, it still allows for efficient manipulation of the model.

In the rest of the paper, we assume that a whitebox attacker has access to the model under attack and can compute its loss directly. We also present a blackbox attacker, where we assume no access to the model. Neither attack makes any prior assumptions about the underlying data.

¹Indeed, occasionally one finds discussions of bad model performance because of data sampling bias or pseudo-randomness problems *e.g.* https://www.reddit.com/r/MachineLearning/comments/mocpgj/p_using_pytorch_numpy_a_bug_that_plagues/

2.2 Threat model

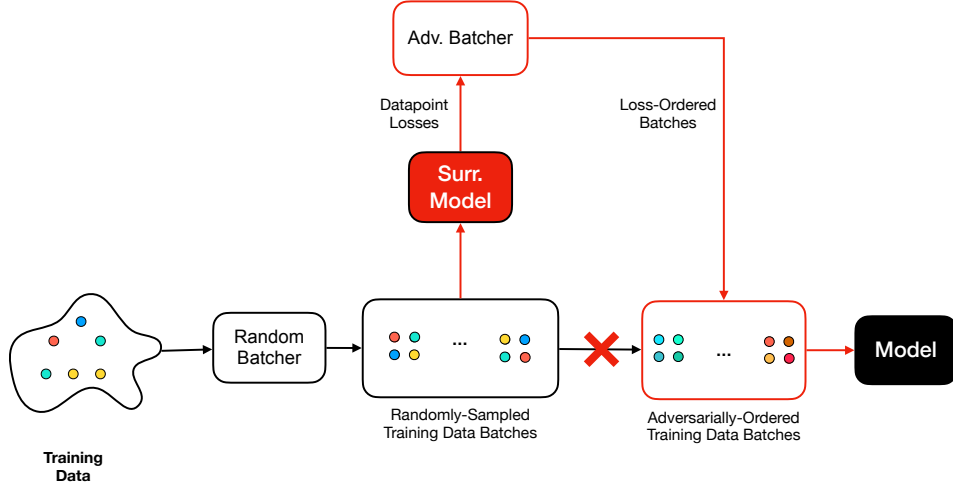


Figure 1: The attacker reorders the benign randomly supplied data based on the surrogate model outputs. The surrogate model is operated by the attacker, who co-trains it with the same data that is supplied to the source model.

We assume one of the strongest threat models currently described in the literature. In particular, our blackbox attacker assumes no access to the model and no prior knowledge of the training data. The attack specifically focuses on the batching part of the ML pipeline as is depicted in Figure 1.

This attack is entirely realistic and can be instantiated in several ways. The attack code can be infiltrated into: the operating system handling file system requests; the disk handling individual data accesses; the software that determines the way random data sampling is performed; the distributed storage manager; or the machine learning pipeline itself handling prefetch operations. That is a substantial attack surface, and for large models these components may be controlled by different principals. The attack is also very stealthy. The attacker does not add any noise or perturbation to the data. There are no triggers or backdoors introduced into the dataset. All of the data points are natural. In two of four variants the attacker uses the whole dataset and does not oversample any given point, *i.e.* the sampling is without replacement. This makes it difficult to deploy simple countermeasures against our attacker.

2.3 Primer on stochastic learning and batching

We assume that the defender is trying to train a deep neural network model with parameters θ operating over $X_i \sim \mathcal{X}_{\text{train}}$, solving a non-convex optimization problem with respect to parameters θ , corresponding to minimization of a given loss function $L(\theta)$. We will denote the training dataset $X = \{X_i\}$. We assume a commonly-used loss function defined as the sample average of the loss per training data point $L_i(\theta) = L(X_i, \theta)$ in k -th batch over the training set, where B is the batch size:

$$\hat{L}_{k+1}(\theta) = \frac{1}{B} \sum_{i=kB+1}^{kB+B} L_i(\theta). \quad (1)$$

If we let $N \cdot B$ be the total number of items sampled for training, then in a single epoch one aims to optimize the function:

$$\hat{L}(\theta) = \frac{1}{N} \sum_{i=1}^N \hat{L}_i(\theta). \quad (2)$$

Optimization with stochastic gradient descent (SGD) algorithm of $N \cdot B$ samples and a learning rate of η leads to the following weight update rule over one epoch:

$$\theta_{k+1} = \theta_k + \eta \Delta \theta_k; \quad \Delta \theta_k = -\nabla_{\theta} \hat{L}_k(\theta_k). \quad (3)$$

SGD is often implemented with momentum [33, 40], with μ and v representing momentum and velocity respectively:

$$v_{k+1} = \mu v_k + \eta \Delta \theta_k; \quad \theta_{k+1} = \theta_k + v_{k+1}. \quad (4)$$

Given data, SGD’s stochasticity comes from the batch sampling procedure. Mini-batched gradients approximate the true gradients of \hat{L} and the quality of this approximation, as we show in the paper, can vary greatly. In fact, assuming an unbiased sampling procedure, *i.e.* when the k ’th gradient step corresponds to i_k ’th batch with $\mathbb{P}(i_k = i) = 1/N$, in expectation the batch gradient matches the true gradient:

$$\mathbb{E}[\nabla \hat{L}_{i_k}(\theta)] = \sum_{i=1}^N \mathbb{P}(i_k = i) \nabla \hat{L}_i(\theta) = \frac{1}{N} \sum_{i=1}^N \nabla \hat{L}_i(\theta) = \nabla \hat{L}(\theta). \quad (5)$$

Although this happens in expectation, a given batch taken in isolation can be very far from the mean. This variation has been exploited in the literature to aid training: there exists a field responsible for variance reduction techniques for stochastic optimisation [23], curriculum learning [4] and core-set construction [2]. Each area looks at identifying and scheduling data subsets that aid training and give a better true gradient approximation. In this paper, we turn things round and investigate how an attacker can exploit data order to break training.

The explicit stochastic assumption opens a new attack surface for the attacker to influence the learning process. In particular, let us consider the effect of N SGD steps over one epoch [38]:

$$\begin{aligned} \theta_{N+1} &= \theta_1 - \eta \nabla \hat{L}_1(\theta_1) - \eta \nabla \hat{L}_2(\theta_2) - \dots - \eta \nabla \hat{L}_N(\theta_N) \\ &= \theta_1 - \eta \sum_{j=1}^N \nabla \hat{L}_j(\theta_1) + \eta^2 \sum_{j=1}^N \sum_{k < j} \nabla \nabla \hat{L}_j(\theta_1) \nabla \hat{L}_k(\theta_1) + O(N^3 \eta^3). \end{aligned} \quad (6)$$

As we can see, in this case the second order correction term is dependent on the order of the batches provided. The attacker we describe in this paper focuses on manipulating it:

$$\sum_{j=1}^N \sum_{k < j} \nabla \nabla \hat{L}_j(\theta_1) \nabla \hat{L}_k(\theta_1), \quad (7)$$

i.e. finding a sequence of updates such that the first and second derivatives are misaligned with the true gradient step. A slightly different choice of an objective here can also enable targeting of the upper bound on the rate of SGD convergence explicitly, which we show in Appendix A.

In this paper we assume the blackbox attacker has no access to the underlying model, and thus no way to monitor its errors or the progress of its training. Instead, we co-train a separate surrogate model, using the batches supplied to the target model. We find that in practice the losses produced by the surrogate model approximate the losses of the true model well enough to enable attacks on both integrity and availability. We demonstrate that our blackbox attack performs as well as the whitebox one in Section 3.2.

Finally, although the attacker can maximise Equation (7) directly, in practice it is expensive to do so. Therefore, in the attack we make use of the loss magnitudes directly. Intuitively, large prediction errors correspond to large loss gradient norms, whereas correct predictions produce near-zero gradients.

2.4 Taxonomy of batching attacks

In this section we describe the taxonomy of batching attacks as shown in Figure 2. The overall attack algorithm is shown in Algorithm 2 in the Appendix, and a shortened attack flow is shown in Algorithm 1. We compare our attacks with the related literature in Section 4.2 and highlight that our attacks are the first to successfully poison the underlying model without changing the underlying dataset.

Batch reshuffling or inter-batch mixing Here, the attacker focuses on changing the order in which individual datapoints appear across the batches in a given epoch.

Batch reordering or intra-batch mixing Here, the attacker focuses on changing the order in which pre-packaged randomly sampled batches get supplied to the model.

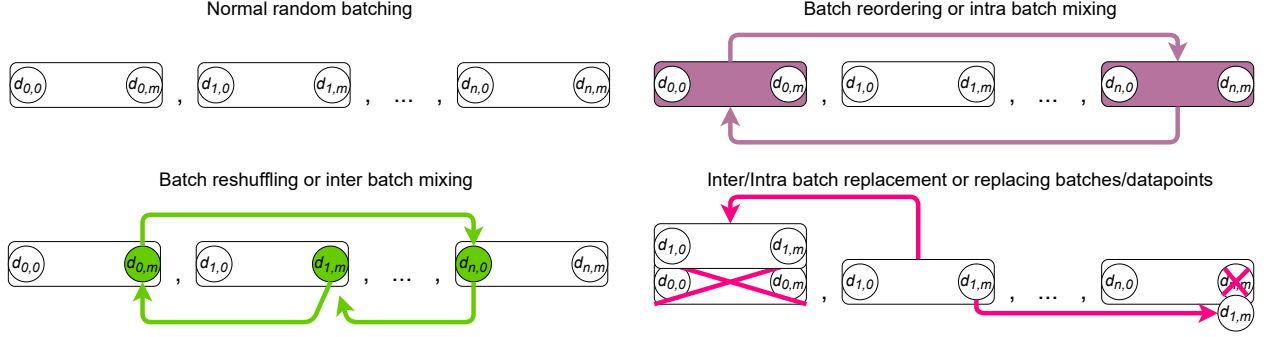


Figure 2: Taxonomy of BRRR attacks. Normal batching assumes randomly distributed data points and batches. Batch reordering assumes the batches appear to the model in a different order, but internal contents stay in the original random order. Batch reshuffling assumes that the individual datapoints within batches change order, but appear only once and do not repeat across batches. Finally, batch replacement refers to cases where individual datapoints or batches can repeat or not appear in an epoch at all.

Algorithm 1: A high level description of the BRRR attack algorithm

```

/* - Attack preparation: collecting data - */
do
    get new batch()
    add to a list of unseen datapoints
    train surrogate model on a batch and pass it on to the model
while first epoch is not finished
/* -- */

/* - Attack : reorder based on surrogate loss - */
while training do
    rank each data point observed in epoch one with a surrogate loss
    reorder the data points according to the attack strategy
    one by one pass batches to model
    train the surrogate on the same batches
/* -- */

```

Data point or batch replacement Here, the attacker focuses on either replacing data points inside of the batches or the whole batches. In this case, an attacker can both over-sample and under-sample the data points.

Now that we have established three ways of attacking batching – changing the order of datapoints inside batches, changing the order of batches, and replacing both points and batches – we turn to reordering itself. We consider four reordering policies, motivated by research in the fields of curriculum learning [4] and core-set selection [2], which discovered that model training can be enhanced by scheduling how and what data is presented to the model. That can help the model to generalize and to avoid overfitting with memorization. This paper does the opposite – we promote memorization and overfitting, forcing the model to forget generalizable features.

Figure 3 shows the different reorder policies that are employed in the paper. **Low to high** orders sequence items by their loss. **High to low** is an inverse of Low to high. **Oscillations inwards** picks elements from both sides in sequence. **Oscillations outwards** inverts the halves of the sequence and then picks elements from both sides.

2.5 Batch-order poison and backdoor

Machine-learning poisoning and backdooring techniques aim to manipulate the training of a given model to control its behavior during inference. In the classical setting, poisoning involves either appending adversarial datapoints \hat{X} to natural dataset X or changing natural datapoints $X + \delta$ so as to change model behaviour. For example, an adversary may add a red pixel above every tank in the dataset to introduce the red pixel trigger and cause other objects under red pixels to be classified as tanks. Both cases require the adversary to modify the training dataset, which makes the attack easier to detect, and to prevent.

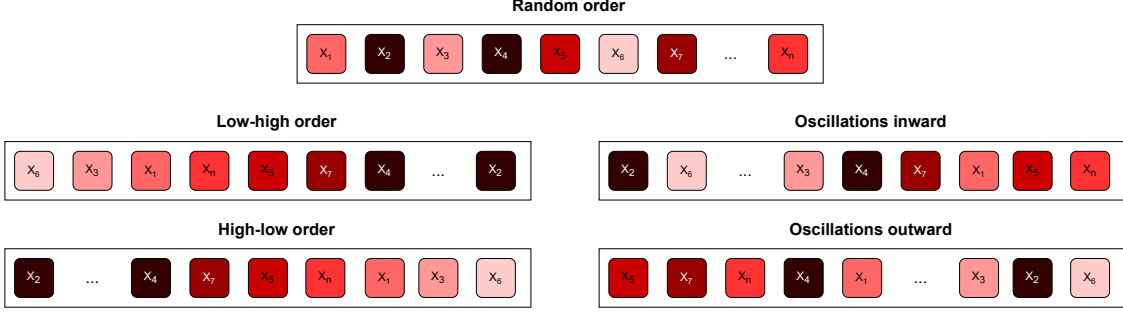


Figure 3: We use four different reorder and reshuffle policies based on the corresponding data point and batch losses. We color-code the loss values from bright to dark colors, to represent loss values from low to high. **Low-high** policy orders a sequence by the loss magnitude. **High-low** policy orders a sequence by the negative loss magnitude. **Oscillation inwards** orders elements of the sequence from the beginning and the end of the sequence one by one, as if it was oscillating between sides of the sequence and moving towards the middle. Finally, **Oscillations outward** orders the sequence by starting at the middle of an ordered sequence picking elements to both sides of the current location.

In this section we discuss batch replacement attacks – the only attacks presented in this paper that can sample the underlying dataset with replacement. We present batch-order poisoning (BOP) and batch-order backdooring (BOB) – the first poison and backdoor strategies that do not rely on adding adversarial datapoints or perturbations during training, but only on changing the order in which genuine data are presented.

BOP and BOB are based on the idea that the stochastic gradient update rule used in DNN training is agnostic of the batch contents and is an aggregation. Indeed, consider a classical poison setting with an adversarial dataset \hat{X} :

$$\theta_{k+1} = \theta_k + \eta \Delta \theta_k; \quad \Delta \theta_k = -(\nabla_{\theta} \hat{L}(X_k, \theta_k) + \nabla_{\theta} \hat{L}(\hat{X}_k, \theta_k)). \quad (8)$$

Order-agnostic aggregation with a sum makes it hard to reconstruct the individual datapoints X_k from just observing $\Delta \theta_k$. Indeed, the stochastic nature of optimisation allows one to find a set of datapoints $X_j \neq X_i$ such that $\nabla_{\theta} \hat{L}(X_i, \theta_k) \approx \nabla_{\theta} \hat{L}(X_j, \theta_k)$.

Given a model and a dataset such that the gradient covariance matrix is non-singular, an attacker can approximate the gradient update from an adversarial dataset \hat{X} using natural datapoints from the genuine dataset X , enabling poisoning without having to change of underlying dataset in any way:

$$\theta_{k+1} = \theta_k + \eta \hat{\Delta} \theta_k, \text{ where } \begin{cases} \hat{\Delta} \theta_k = -\nabla_{\theta} \hat{L}(X_i, \theta_k) \\ \nabla_{\theta} \hat{L}(X_i, \theta_k) \approx \nabla_{\theta} \hat{L}(\hat{X}_k, \theta_k). \end{cases} \quad (9)$$

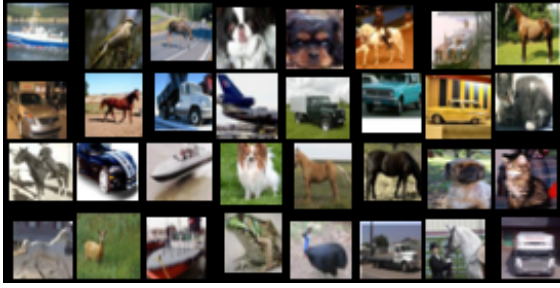
We discuss the fidelity of such reconstructions in Appendix B.

This gives rise to a surprisingly powerful adversary, who can introduce arbitrary behaviors into any models learned with stochastic gradient descent without having to add or perturb training data. This attack becomes better as training datasets become larger, further improving the attacker’s ability to shape the gradient update.

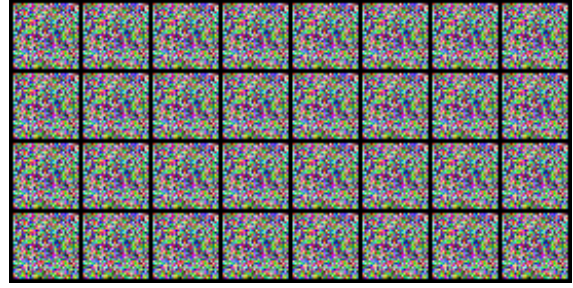
We evaluated a number of different setups, and found that the attack works best when the attacker comprises the batch with $B - V$ natural data points (a larger V is better for gradient approximation, but leads to more conflict with natural gradients; in the paper up to 30% of the batch is filled with natural datapoints to find a balance) and appends V adversarially-chosen data points \hat{X}_i to the batch. Finding precise batch reconstruction is an intractable problem that scales with batch size and size of the dataset with overall $|X|^B$ possible combinations. However, we find that random sampling works well; even if mistakes are made, the network still learns the poison over the course of a few batches. Overall we try to minimize the following reconstruction error for a given poisoned batch \hat{X}_j :

$$\min_{X_i} \left\| \nabla_{\theta} \hat{L}(\hat{X}_j, \theta_k) - \nabla_{\theta} \hat{L}(X_i, \theta_k) \right\|^p; \quad \text{s.t. } X_i \in X. \quad (10)$$

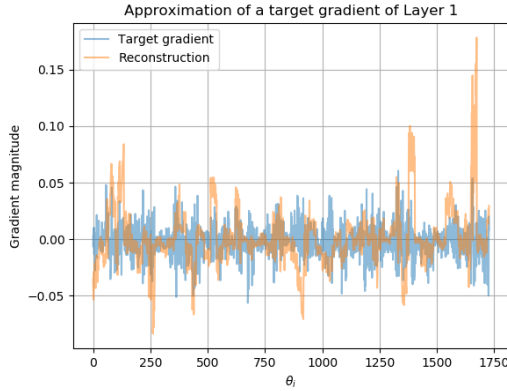
Although more sophisticated approaches could help finding better candidates, we find that random sampling works well enough for successful clean-data / clean-label poison and backdoor attacks. It also helps us strike a balance between



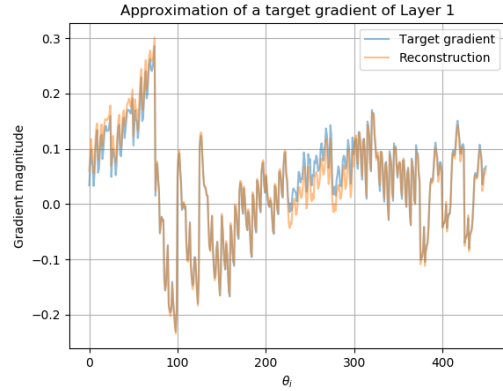
(a) Natural image batch



(b) Poison datapoint batch



(c) Gradients of Layer 1 in the ResNet-18 network. Strong gradients are aligned across the layers and the resulting parameter update successfully changes the prediction of poison datapoints to the label of choice. The network is attacked mid-way training at epoch 10 when it gets to around 80% accuracy.



(d) An example of an almost perfect parameter update reconstruction with a LeNet5 network.

Figure 4: Examples of batches shown in (a) and (b) with very similar gradient updates shown in (c) and (d).

speed of batch construction and impact on model performance. Figure 4 shows an example of a parameter update (c) with natural data presented in (a) that closely resembled the would-be update with batch in (b). More importantly, such update results in a prediction change for data shown in (b) of the base model towards the target class.

It is worth noting that (c) approximation of the gradient is noisy, and it is an artifact of both the model and the data involved in the approximation. In (d) we show an approximation for LeNet-5 model, where the reconstructed approximation quality is significantly higher.

3 Evaluation

3.1 Experimental setup

We evaluate our attacks using the CIFAR-10 and CIFAR-100 datasets [25]. We use ResNet-18 and ResNet-50 as source models [18], and LeNet-5 [26] and MobileNet [20] as surrogate models, to train CIFAR-10 and CIFAR-100 respectively. Note that the surrogate model is significantly less performant than its corresponding source model in both cases, and cannot learn the dataset to the same degree of accuracy. This implies the attacker’s capabilities are limited, ensuring the attack is realistic. Thus our results represent a lower bound on attack performance.

3.2 Integrity attacks in white and blackbox setups

In this section we evaluate the performance of reordering attacks in the whitebox and blackbox settings. In the whitebox case, we assume that the attacker can compute the loss directly to perform the attacks. We show the results in Figure 5.

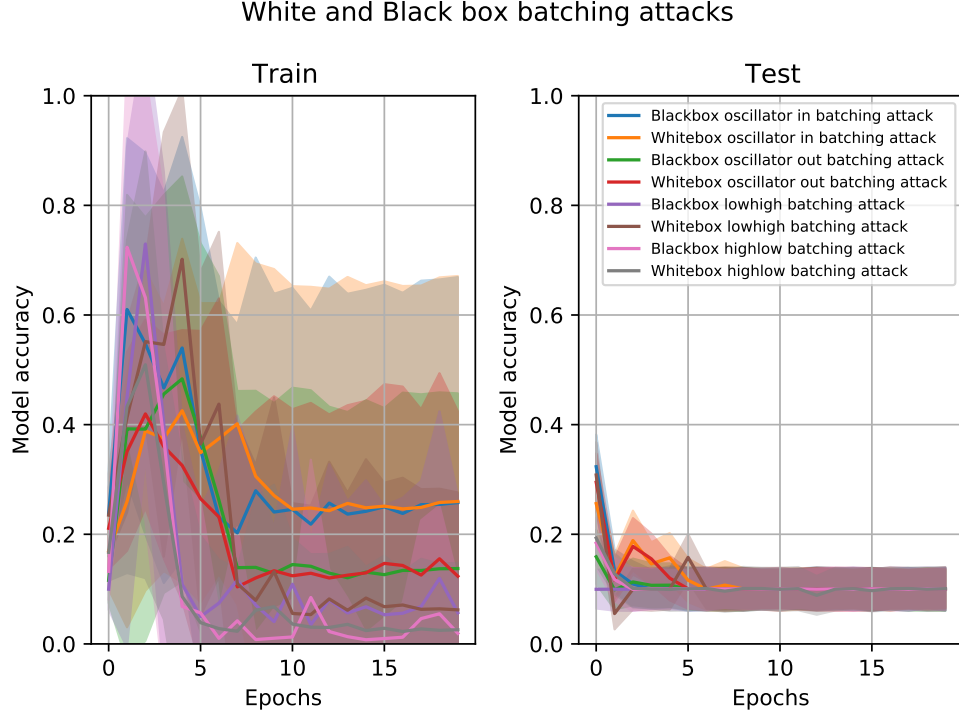


Figure 5: Comparison of White and Blackbox attacks against ResNet-18 network and CIFAR-10 dataset. Error bars shown standard deviation of per-batch accuracy.

Attacks in both settings significantly reduce model accuracy at train-and-test time. Importantly, we observe that both blackbox and whitebox attacks significantly degrade model accuracy, with the blackbox attack also having a smaller standard deviation, demonstrating that the batching attacker is a realistic threat. We show more results in Appendix E and Figure 25.

3.3 Integrity attacks with reshuffling and reordering of natural data

Table 1 presents the results from three kinds of attack presented in the paper evaluated over the CIFAR10 dataset with ResNet18 target model and LeNet5 surrogate model, and CIFAR100 dataset with ResNet50 target model and Mobilenet surrogate model, trained with SGD with 0.3 moment and Adam respectively. Batch reordering disrupts normal model training and introduces from $\sim 10\%$ to 15% performance degradation. Note that the attacker does nothing beyond changing the order of the batches; their internal composition is the same. This clearly shows the potency of this attack. Indeed, when we extend the attack to batch reshuffling – where batches get re-arranged internally – performance degrades to that of random guessing. In each, the best-performing models stay at the first epoch, where the attacker still accumulates the dataset used in training. Here, the degradation in performance is maximum – all models with all attack types failed to perform better than random guessing, having reached their top performance only in the first epoch, when the attacker was observing the dataset.

We additionally report a large number of different hyperparameter variations for the attacks in Appendix D. Hyperparameter search seem to suggest that the attacks work well as long as the surrogate models learn, do not converge to a minimum straight away and have sufficient learning rate.

Overall, we find that:

- An attacker can affect integrity of model training by changing order of individual data items and natural batches.
- The attacker can reduce model performance, and completely reset its performance.

CIFAR-10							CIFAR-100				
Attack	Batch size	Train		Test		Accuracy Δ	Train		Test		Accuracy Δ
		Loss	Accuracy	Loss	Accuracy		Loss	Accuracy	Loss	Accuracy	
<i><u>Baseline</u></i>											
None	32	0.13	95.51	0.42	90.51	−0.0%	0.00	99.96	2.00	75.56	−0.0%
	64	0.09	96.97	0.41	90.65	−0.0%	0.00	99.96	2.30	74.05	−0.0%
	128	0.07	97.77	0.56	89.76	−0.0%	0.00	99.98	1.84	74.45	−0.0%
<i><u>Batch reorder</u></i>											
Oscillation outward	32	0.02	99.37	2.09	78.65	−11.86%	0.00	100.00	5.24	53.05	−22.51%
	64	0.01	99.86	2.39	78.47	−12.18%	0.00	100.00	4.53	55.91	−18.14%
	128	0.01	99.64	2.27	77.52	−12.24%	0.00	100.00	3.22	52.13	−22.32%
Oscillation inward	32	0.01	99.60	2.49	78.18	−12.33%	0.00	100.00	5.07	51.78	−23.78%
	64	0.01	99.81	2.25	79.59	−11.06%	0.00	100.00	4.70	55.05	−19.0%
	128	0.02	99.39	2.23	76.13	−13.63%	0.00	100.00	3.46	52.66	−21.79%
High Low	32	0.02	99.44	2.03	79.65	−10.86%	0.00	100.00	5.47	51.48	−24.08%
	64	0.02	99.50	2.39	77.65	−13.00%	0.00	100.00	5.39	55.63	−18.42%
	128	0.02	99.47	2.80	74.73	−15.03%	0.00	100.00	3.36	53.63	−20.82%
Low High	32	0.01	99.58	2.33	79.07	−11.43%	0.00	100.00	4.42	54.04	−21.52%
	64	0.01	99.61	2.40	76.85	−13.8%	0.00	100.00	3.91	54.82	−19.23%
	128	0.01	99.57	1.88	79.82	−9.94%	0.00	100.00	3.72	49.82	−24.63%
<i><u>Batch reshuffle</u></i>											
Oscillation outward	32	2.26	17.44	1.93	26.13	−64.38%	0.01	99.80	5.01	18.00	−57.56%
	64	2.26	18.86	1.98	26.74	−63.91%	0.38	93.04	4.51	11.68	−62.37%
	128	2.50	14.02	2.18	20.01	−69.75%	0.66	86.22	4.07	10.66	−63.79%
Oscillation inward	32	2.13	22.85	1.93	28.94	−61.57%	0.01	99.92	4.55	31.38	−44.18%
	64	2.27	17.90	1.99	23.59	−67.06%	0.02	99.64	5.79	17.37	−56.68%
	128	2.53	10.40	2.29	13.49	−76.27%	0.54	88.60	4.03	10.92	−63.53%
High Low	32	2.11	23.39	1.80	31.04	−59.47%	0.01	99.69	6.24	21.15	−54.41%
	64	2.22	20.57	1.93	27.60	−63.05%	0.05	99.15	5.26	14.05	−60.0%
	128	2.51	16.66	2.05	20.85	−68.91%	4.16	7.21	3.86	10.20	−64.25%
Low High	32	2.17	20.22	1.92	30.09	−60.42%	0.19	96.07	4.06	20.48	−55.08%
	64	2.35	15.98	2.00	22.97	−67.68%	0.09	98.22	4.69	15.39	−58.66%
	128	2.51	10.25	2.32	11.40	−78.36%	4.30	5.65	3.81	9.66	−64.79%

Table 1: For CIFAR-10, we used 100 epochs of training with target model ResNet18 and surrogate model LeNet5, both trained with the Adam optimizer and $\beta = (0.99, 0.9)$. For CIFAR-100, we used 200 epochs of training with target model ResNet50 and surrogate model Mobilenet, trained with SGD with 0.3 moment and Adam respectively for real and surrogate models. We highlight models that perform best in terms of test dataset loss. Numbers here are from best-performing model test loss-wise. Incidentally, best performance of all models for Batch reshuffle listed in the table happen at epoch number one, where the attacker is preparing the attack and is collecting the training dataset. All attacks result in near-random guess performance for almost all subsequent epochs.

3.4 Availability attacks

While the previous section discussed integrity attacks, this section’s focus is on availability. This refers to the amount of time and effort required to train a model, and an availability attack can involve an adversary using BRRR attacks to slow down training without disrupting the overall learning procedure. It is worth noting that there are other possible definitions of availability; it can also mean a model’s ability to reach original accuracy, but this case is already included in the integrity attacks we discussed in the last section.

Availability attacks follow a similar scenario to Section 3.3 above, in that the attacker only changes the order in which data reaches the model. Here we at the 10th epoch, an arbitrary attack point, and all other training is done with randomly ordered data. We find that by feeding the model with a few BRRR batches, its training progress can be reset significantly – progress that may take a surprisingly large number of epochs to recover. The red line shows the worst possible scenario, where each batch has only data points of a single class. It can be seen that the attack manages to reset training, degrading performance for more than 90 epochs – low-high batch reordering at epoch ten results in −3% performance at epoch 100.

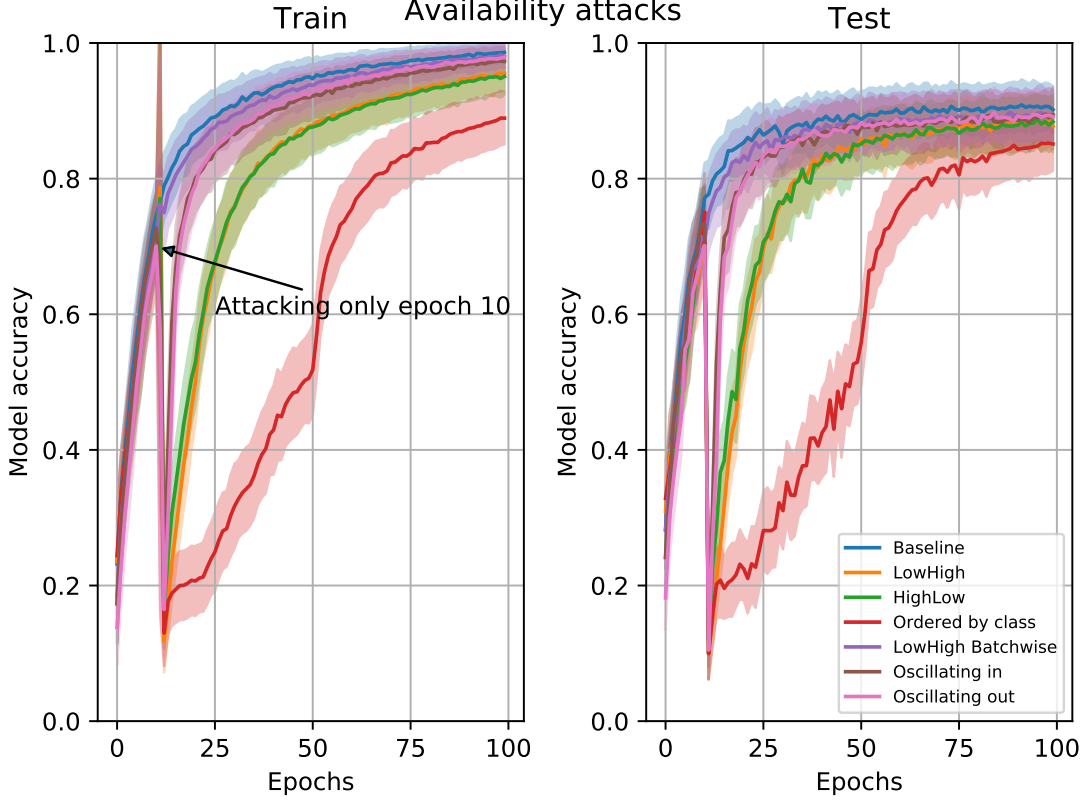


Figure 6: Availability attacks at epoch 10, ResNet-18 attacked with a LeNet-5 surrogate. Error bars show per-batch accuracy standard deviation.

In this section we showed that the attacker can perform availability attacks using both batch reordering and reshuffling. We find that BRRR attacks end up having an impact on a model long after they have been launched and do not need to happen every step; even a single attack epoch can degrade training progress significantly.

Overall, we find that:

- An attacker can cause disruption to model training by changing the order of data in just a single epoch of training.
- An attack at just one epoch is enough to degrade the training for more than 90 epochs.

3.5 BOP and BOB with batch replacement

Single datapoint poison: Here we train the network with clean data for 10 epochs, and then start injecting 95 BOP batches to poison a single random datapoint. We find that poisoned datapoints converge relatively quickly to the target class. Figure 7 shows the performance of a single-datapoint poison for four different architectures. In each a fixed random target point ends up getting the target class after a few batches. For all but one, the point ends up getting to the target class within 10 batches; for VGG-16 it took around 50.

Backdooring and trigger construction: We find that the same method as for poison can be used to backdoor the models and control their behavior in presence of a trigger. Here, we apply a trigger to images from the training dataset. We find that our method enables the attacker to control the decision of a model when it makes a mistake *i.e.* when the model is making a decision about data far from the training-set distribution. We hypothesise that the limitation comes from the fact that as only natural data are sampled for each BOP and BOB batch, natural gradients are present and learning continues; so forgetting does not happen and generalisation is not disrupted.

There are two ways forward. First, the model can first be manipulated to unlearn the given datapoint (*e.g.* with Section 3.4). Second, if the trigger is chosen to force the model to make mistakes (*i.e.* model generalisation will not slow

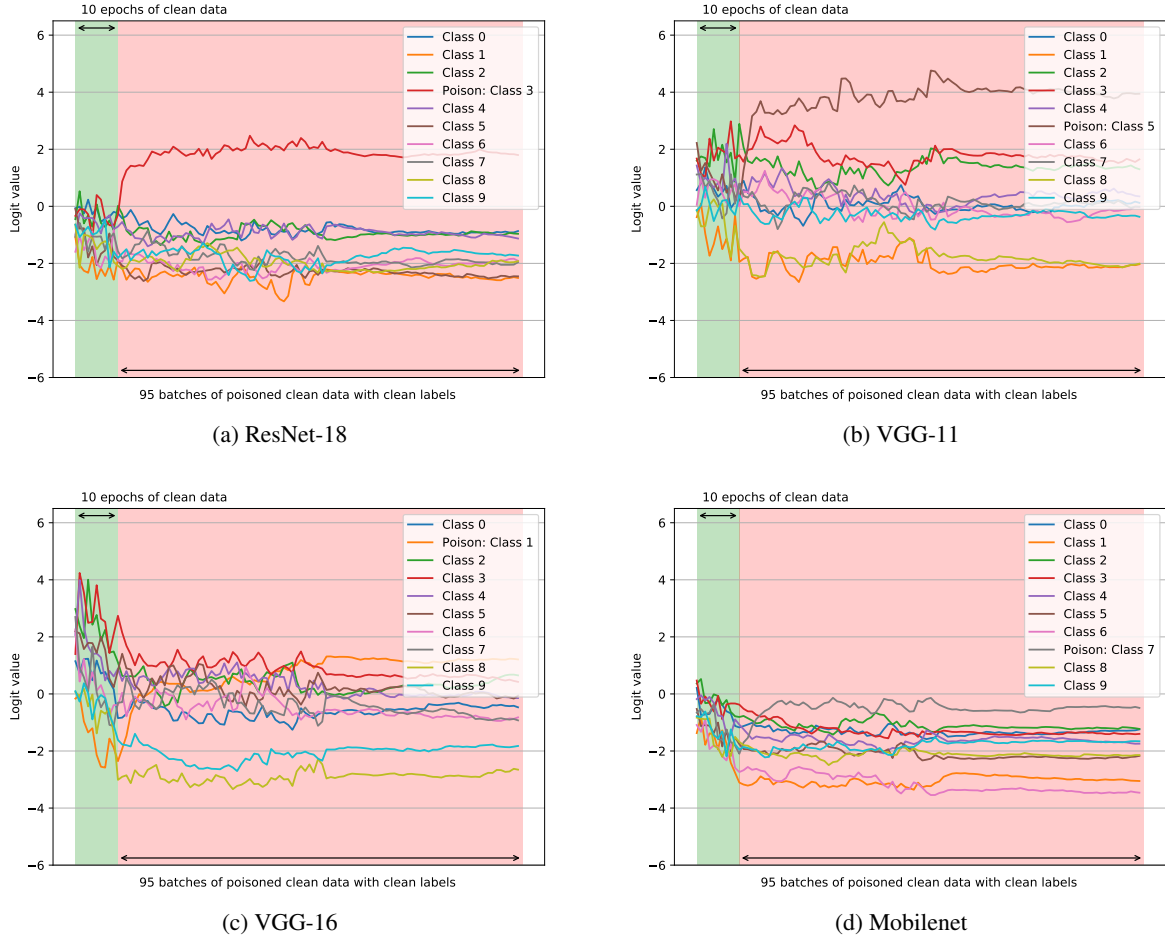


Figure 7: Logit values of a network with 10 epochs of clean data and 95 batches of poisoned data. It takes around 3–5 poison ordered batches for ResNet-18 and VGG-11, 10 for Mobilenet, whereas VGG-16 takes about 50 batches. After poisoning, all models lost at most 10% accuracy.

down gradient shaping), these mistakes can be targeted. We evaluate two examples of such triggers shown in Figure 8, a white lines trigger, which practically clears the top part of an image, or flag-like trigger that spans all of the image. Do note that magnitude-wise both triggers are the same, affecting 30% of the natural image.



Figure 8: Examples of triggers used in the paper.

In the paper we report results from injecting up to 20 adversarially-ordered batches every 50000 natural datapoints for 10 epochs. We then inject 80 adversarially-ordered batches. The training procedure here is similar to the one used for BadNets [15]. We find that 80 batches are not really required, as most models end up converging after 3–5 adversarially-ordered batches. For reconstruction we randomly sample 300 batches and use $p = 2$.

Table 2 shows BOB trigger performance for both whitebox and blackbox setups. We present two baselines, one for normal training without any triggers, and one where triggers are added to the underlying data, *i.e.* training with

Trigger	Batch size	Train acc [%]	Test acc [%]	Trigger acc [%]	Error with trigger [%]
<i>Baselines</i>					
Random natural data	32	88.43 \pm 7.26	79.60 \pm 1.49	10.91 \pm 1.53	30.70 \pm 2.26
	64	95.93 \pm 2.11	81.31 \pm 2.01	9.78 \pm 1.25	27.38 \pm 1.20
	128	94.92 \pm 2.04	81.69 \pm 1.17	10.00 \pm 2.26	27.91 \pm 1.41
Data with trigger perturbation	32	96.87 \pm 2.79	73.28 \pm 2.93	99.65 \pm 0.22	89.68 \pm 0.21
	64	98.12 \pm 1.53	79.45 \pm 1.39	99.64 \pm 0.21	89.64 \pm 0.21
	128	98.67 \pm 0.99	80.51 \pm 1.10	99.67 \pm 0.40	89.65 \pm 0.39
<i>Only reordered natural data</i>					
9 white lines trigger	32	88.43 \pm 6.09	78.02 \pm 1.50	33.93 \pm 7.37	40.78 \pm 5.70
	64	95.15 \pm 2.65	82.75 \pm 0.86	25.02 \pm 3.78	33.91 \pm 2.28
	128	95.23 \pm 2.24	82.90 \pm 1.50	21.75 \pm 4.49	31.75 \pm 3.68
Blackbox 9 white lines trigger	32	88.43 \pm 4.85	80.84 \pm 1.20	17.55 \pm 3.71	33.64 \pm 2.83
	64	93.59 \pm 3.15	82.64 \pm 1.64	16.59 \pm 4.80	30.90 \pm 3.08
	128	94.84 \pm 2.24	81.12 \pm 2.49	16.19 \pm 4.01	31.33 \pm 3.73
Flag-like trigger	32	90.93 \pm 3.81	78.46 \pm 1.04	91.03 \pm 12.96	87.08 \pm 2.71
	64	96.87 \pm 1.21	82.95 \pm 0.72	77.10 \pm 16.96	82.92 \pm 3.89
	128	95.54 \pm 1.88	82.28 \pm 1.50	69.49 \pm 20.66	82.09 \pm 3.78
Blackbox flag-like trigger	32	86.25 \pm 4.00	80.16 \pm 1.91	56.31 \pm 19.57	78.78 \pm 3.51
	64	95.00 \pm 2.18	83.41 \pm 0.94	48.75 \pm 23.28	78.11 \pm 4.40
	128	93.82 \pm 2.27	81.54 \pm 1.94	68.07 \pm 18.55	81.23 \pm 3.80

Table 2: Performance of triggers induced only with natural data. Network is VGG16 that has been trained normally on CIFAR10 for 10 epochs and then gets attacked with 10 trigger batches. Test accuracy refers to the original benign accuracy, ‘Trigger acc’ is the proportion of images that are classified as the trigger target label, while ‘Error with trigger’ refers to all of the predictions that result in an incorrect label. Standard deviations are calculated over different target classes. Blackbox results use a ResNet-18 surrogate.

perturbed data and labels. Trigger accuracy refers to the proportion of test set that ends up getting the target trigger label, whereas error with triggers shows the proportion of misclassifications that trigger introduces, *i.e.* when the model makes a mistake, but does not predict the trigger target class. As expected, we observe that for normal training, trigger accuracy stays at random guessing, and the trigger does not dominate errors it introduces, whereas adding perturbed data manipulates the model to predict the target class almost perfectly.

We find that in a whitebox setup for a flag-like trigger we are capable of getting a similar order of performance for a batch of size 32 as if the attack was performed with injected adversarial data. In a blackbox setup with a flag-like trigger we lost around 30% of trigger performance, yet the trigger still remains operational. Large standard deviations suggest that the performance depends on a target class of the trigger and we hypothesise that this is connected with the fidelity of gradient reconstruction. A trigger of nine white lines outperforms the baseline only marginally; in a whitebox it gets from 20–40% performance, whereas in a blackbox it ranges between zero and 20% performance. We show the training progress of each individual trigger in Appendix F.

Overall, we find that:

- An attacker can poison an individual datapoint, change its label and increase its prediction confidence, without ever actually showing the model an adversarially-crafted datapoint.
- An attacker can introduce backdoors into the model by introducing a few reordered batches during training, without ever injecting adversarial data or labels. Here, trigger performance differs, yet an adversary can perform BOB attacks on a par with attacks that inject perturbations into datasets explicitly.

Attack	Dataset knowledge	Model knowledge	Model specific	Changing dataset	Adding data	Adding perturbations
Batch Reorder	✗	✗	✗	✗	✗	✗
Batch Reshuffle	✗	✗	✗	✗	✗	✗
Batch Replace	✗	✗	✗	✗	✗	✗
Adversarial initialisation [14]	✗	✓	✓	✗	✗	✗
BadNets [15]	✓	✗	✗	✓	✗	✓
Dynamic triggers [35]	✓	✓	✗	✓	✗	✓
Poisoned frogs [39]	✓	✓	✗	✓	✗	✓

Table 3: Taxonomy of training time integrity attacks. In green, we highlight our attacks.

4 Related Work

4.1 Machine Learning and Batching

Batch gradient descent considers all the data points in the training set to take a single optimization step, but this becomes computationally intractable with large datasets. Stochastic gradient descent computes gradients from a set of selected samples, also known as a minibatch [6, 27]. Previous studies illustrate that batch size can affect the training convergence. Small batches (around 32) help learning to avoid local minima and provide improved generalization performance [30]. Large batch sizes offer a greater data parallelism but often require several learning-rate scaling tricks to ensure convergence [13].

Previous work has also looked at the relationship between BatchNorm [21] statistics and adversarial machine learning. Galloway *et al.* investigated the effects that BatchNorm has on the adversarial robustness of DNNs [10]. Xie *et al.* showed that adversarial samples have a different underlying distribution from normal examples [42].

Another important factor that affects training convergence is model initialisation. The lottery ticket hypothesis shows that certain groups of winning tickets (weight initialisation) make training particularly effective [9]. Work on model initialisation shows that weight variance is of great importance [16, 17]. An attack on the model training phase by targeting model initialization [14] is also possible, and Grosse *et al.* exploit ReLU activation functions to reduce the capacity of the underlying neural networks.

4.2 Adversarial Machine Learning

Attacks on integrity: Szegedy *et al.* [41] and Biggio *et al.* [5] concurrently discovered the existence of adversarial examples. These samples, containing human imperceptible perturbations, cause models to output incorrect results during inference. The original whitebox attacks require the adversary to access the models and use gradient information to perform conditioned optimisation to maximise the model loss [41, 5, 12, 29]. The attack later generalised to blackbox setups, where the adversary trains a surrogate model and hopes the generated adversarial samples transfer to the target model [32].

The data-poisoning attack aims at using data manipulation to cause DNNs to fail on specific test-time instances [22]. Chen *et al.* demonstrated that manipulation of the labels of around 50 training samples is enough to trigger failure [8]. Gu *et al.* showed that attackers can associate adversarial patterns with labelled images and cause DNNs to overfit to this pattern [15]. Shafahi *et al.* launched a poisoning attack using instances with clean labels [36]. A number of other works have since created more efficient triggers [35]. It was a common belief that poisoning attacks on DNNs have to contain a certain level of malicious manipulation of whether the data or label at train time. However, this paper shows how poisoning is possible with clean data and clean labels, with the only manipulation being of the batching process at training time.

Attacks on availability: Shumailov *et al.* first attacked the availability of computer vision and natural language processing models at inference time with sponge examples [37]. They pessimized over energy utilisation and inference latency to target hardware and internal model optimisations.

By contrast, this paper targets availability at training time. We show that the attacker can reset or slow down training progress by reordering or reshuffling natural batches. It is worth noting that our definition of availability is broader than that commonly found in the literature, which misses training slowdowns and resets. In this paper we explore all of the above.

Finally, we note that unlike Shumailov *et al.*, our attacks do not target specific optimisations in hardware or individual models, but instead break the fundamental stochastic assumption of training.

4.3 Failures of randomness

There exists a very substantial security-engineering literature on the failures of random-number generators, particularly in cryptographic applications. Bad random number generators shipped with operating systems have led to the large-scale compromise of cryptographic keys generated with them; in at least one case this was deliberate, when the NSA persuaded NIST to specify the dual-EC random number generator which apparently contained a weakness that the US intelligence community could exploit. Many implementations of the EMV standard for payment card cryptography used an ‘unpredictable number’ that was in fact predictable, leading to fraud. For discussion of such cases, see Anderson [1].

This paper reminds us that stochastic gradient descent, like cryptography, depends on randomness. A random number generator with a backdoor can undermine a neural network just as it can undermine a payment network. The requirement for SGD is not however secrecy, but transparency. Recent work has highlighted that ML models can be racist and suffer from a large taxonomy of different biases, including sampling bias [3, 31]. This leads directly to questions of inductive bias and the practical contribution of pseudorandom sampling. Hooker has explained that bias in ML is not just a data problem, but depends on algorithms in subtle ways [19]; this paper shows how to exploit that dependency.

Developers who wish to ensure secure, robust, fair, and optimized learning must therefore be able to show the provenance of randomness used to select batches and datapoints. Cryptography might help; one can use the AES algorithm to generate a pseudorandom sequence that passes all known statistical tests for randomness, yet is repeatable and thus auditable [1]. But the real hard work will be in the implementation: using techniques such as verification and risk-limiting audits to provide assurance of the whole software toolchain between the pseudorandom generator and the model.

5 Conclusion

In this paper we presented a novel class of attacks that manipulate integrity and availability of model training by changing the order of batches, or the order of datapoints within them. Careful reordering of a model’s training data allows it to be poisoned or backdoored without changing the training data set at all. The attacks we presented are fully blackbox; they do not rely on knowledge of the target model or on prior knowledge of the training data.

Most surprisingly, we find that an attacker can introduce backdoors without disruption of overall model generalisation, even though only natural data is used. Our paper is the first to show that the sampling procedure can be manipulated deterministically to control how the model behaves.

Finally, our work highlights that if we want to build trustworthy machine-learning systems, then we need to base them on pipelines that are safe and secure by default and that allow for inspection. The increasing complexity of large models causes individual components to become hidden from each other, reducing overall transparency. Complexity and opacity will lead to problems and exploitation in the future. One possible way forward is to use cryptography to ensure that the randomness used to drive the selection of datapoints and batches during training is auditable. However the devil will, as always, lie in the detail.

References

- [1] R. Anderson. *Security engineering*. John Wiley & Sons, 2020.
- [2] O. Bachem, M. Lucic, and A. Krause. Practical coresets constructions for machine learning, 2017.
- [3] R. Baeza-Yates. Bias on the web. *Commun. ACM*, 61(6):54–61, May 2018.
- [4] Y. Bengio, J. Louradour, R. Collobert, and J. Weston. Curriculum learning. In *Proceedings of the 26th Annual International Conference on Machine Learning*, ICML ’09, page 41–48, New York, NY, USA, 2009. Association for Computing Machinery.
- [5] B. Biggio, I. Corona, D. Maiorca, B. Nelson, N. Šrndić, P. Laskov, G. Giacinto, and F. Roli. Evasion attacks against machine learning at test time. In *Joint European conference on machine learning and knowledge discovery in databases*, pages 387–402. Springer, 2013.
- [6] L. Bottou. Large-scale machine learning with stochastic gradient descent. In *Proceedings of COMPSTAT’2010*, pages 177–186. Springer, 2010.
- [7] T. Brown, B. Mann, N. Ryder, M. Subbiah, J. D. Kaplan, P. Dhariwal, A. Neelakantan, P. Shyam, G. Sastry, A. Askell, S. Agarwal, A. Herbert-Voss, G. Krueger, T. Henighan, R. Child, A. Ramesh, D. Ziegler, J. Wu, C. Winter, C. Hesse, M. Chen, E. Sigler, M. Litwin, S. Gray, B. Chess, J. Clark, C. Berner, S. McCandlish, A. Radford, I. Sutskever, and D. Amodei. Language models are few-shot learners. In H. Larochelle, M. Ranzato,

- R. Hadsell, M. F. Balcan, and H. Lin, editors, *Advances in Neural Information Processing Systems*, volume 33, pages 1877–1901. Curran Associates, Inc., 2020.
- [8] X. Chen, C. Liu, B. Li, K. Lu, and D. Song. Targeted backdoor attacks on deep learning systems using data poisoning. *arXiv preprint arXiv:1712.05526*, 2017.
 - [9] J. Frankle and M. Carbin. The lottery ticket hypothesis: Finding sparse, trainable neural networks. *arXiv preprint arXiv:1803.03635*, 2018.
 - [10] A. Galloway, A. Golubeva, T. Tanay, M. Moussa, and G. W. Taylor. Batch normalization is a cause of adversarial vulnerability, 2019.
 - [11] X. Gao, Y. Zhao, Ł. Dudziak, R. Mullins, and C.-z. Xu. Dynamic channel pruning: Feature boosting and suppression. *arXiv preprint arXiv:1810.05331*, 2018.
 - [12] I. J. Goodfellow, J. Shlens, and C. Szegedy. Explaining and harnessing adversarial examples, 2015.
 - [13] P. Goyal, P. Dollár, R. Girshick, P. Noordhuis, L. Wesolowski, A. Kyrola, A. Tulloch, Y. Jia, and K. He. Accurate, large minibatch sgd: Training imagenet in 1 hour. *arXiv preprint arXiv:1706.02677*, 2017.
 - [14] K. Grosse, T. A. Trost, M. Mosbach, M. Backes, and D. Klakow. On the security relevance of initial weights in deep neural networks. In I. Farkaš, P. Masulli, and S. Wermter, editors, *Artificial Neural Networks and Machine Learning – ICANN 2020*, pages 3–14, Cham, 2020. Springer International Publishing.
 - [15] T. Gu, B. Dolan-Gavitt, and S. Garg. Badnets: Identifying vulnerabilities in the machine learning model supply chain. *arXiv preprint arXiv:1708.06733*, 2017.
 - [16] B. Hanin. Which neural net architectures give rise to exploding and vanishing gradients?, 2018.
 - [17] B. Hanin and D. Rolnick. How to start training: The effect of initialization and architecture, 2018.
 - [18] K. He, X. Zhang, S. Ren, and J. Sun. Deep residual learning for image recognition. In *Proceedings of the IEEE conference on computer vision and pattern recognition*, pages 770–778, 2016.
 - [19] S. Hooker. Moving beyond “algorithmic bias is a data problem”. *Patterns*, 2(4):100241, 2021.
 - [20] A. G. Howard, M. Zhu, B. Chen, D. Kalenichenko, W. Wang, T. Weyand, M. Andreetto, and H. Adam. Mobilenets: Efficient convolutional neural networks for mobile vision applications. *arXiv preprint arXiv:1704.04861*, 2017.
 - [21] S. Ioffe and C. Szegedy. Batch normalization: Accelerating deep network training by reducing internal covariate shift. In *International conference on machine learning*, pages 448–456. PMLR, 2015.
 - [22] M. Jagielski, A. Oprea, B. Biggio, C. Liu, C. Nita-Rotaru, and B. Li. Manipulating machine learning: Poisoning attacks and countermeasures for regression learning. In *2018 IEEE Symposium on Security and Privacy (SP)*, pages 19–35. IEEE, 2018.
 - [23] R. Johnson and T. Zhang. Accelerating stochastic gradient descent using predictive variance reduction. *Advances in neural information processing systems*, 26:315–323, 2013.
 - [24] N. P. Jouppi, C. Young, N. Patil, D. Patterson, G. Agrawal, R. Bajwa, S. Bates, S. Bhatia, N. Boden, A. Borchers, et al. In-datacenter performance analysis of a tensor processing unit. In *Proceedings of the 44th Annual International Symposium on Computer Architecture*, pages 1–12, 2017.
 - [25] A. Krizhevsky, G. Hinton, et al. Learning multiple layers of features from tiny images. 2009.
 - [26] Y. LeCun, L. Bottou, Y. Bengio, and P. Haffner. Gradient-based learning applied to document recognition. *Proceedings of the IEEE*, 86(11):2278–2324, 1998.
 - [27] M. Li, T. Zhang, Y. Chen, and A. J. Smola. Efficient mini-batch training for stochastic optimization. In *Proceedings of the 20th ACM SIGKDD international conference on Knowledge discovery and data mining*, pages 661–670, 2014.
 - [28] H. Liu, K. Simonyan, and Y. Yang. Darts: Differentiable architecture search. *International Conference on Learning Representations (ICLR)*, 2019.
 - [29] A. Madry, A. Makelov, L. Schmidt, D. Tsipras, and A. Vladu. Towards deep learning models resistant to adversarial attacks, 2019.
 - [30] D. Masters and C. Luschi. Revisiting small batch training for deep neural networks, 2018.
 - [31] N. Mehrabi, F. Morstatter, N. Saxena, K. Lerman, and A. Galstyan. A survey on bias and fairness in machine learning. *CoRR*, abs/1908.09635, 2019.
 - [32] N. Papernot, P. McDaniel, I. Goodfellow, S. Jha, Z. B. Celik, and A. Swami. Practical black-box attacks against machine learning. In *Proceedings of the 2017 ACM on Asia conference on computer and communications security*, pages 506–519, 2017.

- [33] B. Polyak. Some methods of speeding up the convergence of iteration methods. *USSR Computational Mathematics and Mathematical Physics*, 4(5):1–17, 1964.
- [34] H. Robbins and S. Monro. A stochastic approximation method. *The annals of mathematical statistics*, pages 400–407, 1951.
- [35] A. Salem, R. Wen, M. Backes, S. Ma, and Y. Zhang. Dynamic backdoor attacks against machine learning models, 2020.
- [36] A. Shafahi, W. R. Huang, M. Najibi, O. Suciu, C. Studer, T. Dumitras, and T. Goldstein. Poison frogs! targeted clean-label poisoning attacks on neural networks. *arXiv preprint arXiv:1804.00792*, 2018.
- [37] I. Shumailov, Y. Zhao, D. Bates, N. Papernot, R. Mullins, and R. Anderson. Sponge examples: Energy-latency attacks on neural networks. In *6th IEEE European Symposium on Security and Privacy (EuroS&P)*, 2021.
- [38] S. L. Smith, B. Dherin, D. G. T. Barrett, and S. De. On the origin of implicit regularization in stochastic gradient descent, 2021.
- [39] M. Sun, S. Agarwal, and J. Z. Kolter. Poisoned classifiers are not only backdoored, they are fundamentally broken, 2020.
- [40] I. Sutskever, J. Martens, G. Dahl, and G. Hinton. On the importance of initialization and momentum in deep learning. In S. Dasgupta and D. McAllester, editors, *Proceedings of the 30th International Conference on Machine Learning*, volume 28 of *Proceedings of Machine Learning Research*, pages 1139–1147, Atlanta, Georgia, USA, 17–19 Jun 2013. PMLR.
- [41] C. Szegedy, W. Zaremba, I. Sutskever, J. Bruna, D. Erhan, I. Goodfellow, and R. Fergus. Intriguing properties of neural networks. *arXiv preprint arXiv:1312.6199*, 2013.
- [42] C. Xie, M. Tan, B. Gong, J. Wang, A. L. Yuille, and Q. V. Le. Adversarial examples improve image recognition. In *Proceedings of the IEEE/CVF Conference on Computer Vision and Pattern Recognition*, pages 819–828, 2020.

A Stochastic gradient descent and rate of convergence

In this section we are going to investigate the effect of the attack through a prism of a biased gradient estimator on the general analysis and bounds for stochastic gradient descent, presented by Robbins and Monroe [34]. For functions \hat{L}_i that are strongly convex and Lipschitz continuous with Lipschitz constant M , the SGD update rule for a random selection of batch i_k from $\{1, 2, \dots, N\}$ is:

$$\theta_{k+1} = \theta_k - \eta_k \nabla \hat{L}_{i_k}(\theta_k).$$

Assuming $\mathbb{P}(i_k = i) = \frac{1}{N}$, the stochastic gradient is an unbiased estimate of the gradient :

$$\mathbb{E}[\nabla \hat{L}_{i_k}(w)] = \sum_{i=1}^N \mathbb{P}(i_k = i) \nabla \hat{L}_i(w) = \frac{1}{N} \sum_{i=1}^N \nabla \hat{L}_i(w) = \nabla \hat{L}(w).$$

A bound can be computed under the assumption of Lipschitz continuity of $\nabla \hat{L}$

$$\hat{L}(\theta_{k+1}) \leq \hat{L}(\theta_k) + \nabla \hat{L}(\theta_k)^\top (\theta_{k+1} - \theta_k) + \frac{M}{2} \|\theta_{k+1} - \theta_k\|^2, \quad (11)$$

where M is the Lipschitz constant. By the SGD update rule:

$$\hat{L}(\theta_{k+1}) \leq \hat{L}(\theta_k) + \eta_k \nabla \hat{L}(\theta_k)^\top \nabla \hat{L}_{i_k}(\theta_k) + \eta_k^2 \frac{M}{2} \left\| \nabla \hat{L}_{i_k}(\theta_k) \right\|^2. \quad (12)$$

And for an unbiased batch choice, the equation turns into:

$$\mathbb{E}[\hat{L}(\theta_{k+1})] \leq \hat{L}(\theta_k) - \eta_k \left\| \nabla \hat{L}(\theta_k) \right\|^2 + \eta_k^2 \frac{M}{2} \mathbb{E} \left\| \nabla \hat{L}_{i_k}(\theta_k) \right\|^2. \quad (13)$$

Leading to the final bound, which looks like:

$$\min_{k=1, \dots, t} \mathbb{E} \left\| \nabla \hat{L}(\theta_k) \right\|^2 \leq \frac{\hat{L}(\theta_1) - \hat{L}^*}{\sum_{k=1}^t \eta_k} + \frac{M}{2} \frac{\sum_{k=1}^t \eta_k^2 \mathbb{E} \left\| \nabla \hat{L}_{i_k}(\theta_k) \right\|^2}{\sum_{k=1}^t \eta_k}. \quad (14)$$

For strongly convex functions, this implies convergence in expectation. But assuming biased batch sampling we have an extra term:

$$\min_{k=1, \dots, t} \mathbb{E} \left\| \nabla \hat{L}(\theta_k) \right\|^2 \leq \quad (15)$$

$$\frac{\hat{L}(\theta_1) - \hat{L}^*}{\sum_{k=1}^t \eta_k} + \frac{M}{2} \frac{\sum_{k=1}^t \eta_k^2 \mathbb{E} \left\| \nabla \hat{L}_{i_k}(\theta_k) \right\|^2}{\sum_{k=1}^t \eta_k} - \mathbb{E} \left[\frac{\sum_{k=1}^t \eta_k \nabla \hat{L}(\theta_k)^\top \left(\mathbb{E}[\nabla \hat{L}_{i_k}(\theta_k)] - \nabla \hat{L}(\theta_k) \right)}{\sum_{k=1}^t \eta_k} \right]. \quad (16)$$

In our specific setup the step size is fixed, making the bound simpler:

$$\min_{k=1, \dots, t} \mathbb{E} \left\| \nabla \hat{L}(\theta_k) \right\|^2 \leq \frac{\hat{L}(\theta_1) - \hat{L}^*}{\eta t} + \frac{M\eta}{2} \mathbb{E} \left\| \nabla \hat{L}_{i_k}(\theta_k) \right\|^2 - \mathbb{E} \left[\hat{L}(\theta_k)^\top \left(\mathbb{E}[\nabla \hat{L}_{i_k}(\theta_k)] - \nabla \hat{L}(\theta_k) \right) \right]. \quad (17)$$

A biased bound varies from the unbiased one in two terms: $\mathbb{E} \left\| \nabla \hat{L}_{i_k}(\theta_k) \right\|^2$ and $\mathbb{E} \left[\hat{L}(\theta_k)^\top \left(\mathbb{E}[\nabla \hat{L}_{i_k}(\theta_k)] - \nabla \hat{L}(\theta_k) \right) \right]$. The bound will grow if the former term becomes larger, while the latter becomes large and negative.

The first two terms in equation 17 can be made arbitrarily small by a suitable choice of η and t , under an assumption of bounded variance. The last term, on the other hand, does not directly depend on η or t in an obvious way. To be more

Algorithm 2: BRRR attack algorithm

Input: real model M , surrogate model S , loss of model \mathcal{L}_M , loss of surrogate model \mathcal{L}_S , function *getbatch* to get next batch of real data, function *train*(model M' , \mathcal{L} , \mathbf{B}) that trains model M' with loss \mathcal{L} on batch of data \mathbf{B} , current attack type \mathbf{ATK} , batch type attack \mathbf{BTCH} (reorder batchers or reshuffling datapoints)

```

/* List to store data points */
datas = []
/* Let the model to train for a single epoch to record all of the data. */
do
    b = getbatch()
    if BTCH == "batch" then
        | add batch b into datas
    else
        | add individual points from batch b into datas
    train(M,  $\mathcal{L}_M$ , b)
    train(S,  $\mathcal{L}_S$ , b)
while b not in datas
/* Now that all data has been seen, start the attack */
while training do
    /* List to store data-loss of individual points */
    datacosts = {}
    for datapoint or batch d in datas do
        | loss =  $\mathcal{L}_S(S, d)$ 
        | datacosts[d] = loss
    /* List to store data points or batches not yet used in the current epoch, sorted from low to high loss */
    epochdatas = copy(datas).sort(by datacosts)
    if ATK == "oscillating out" then
        /* If oscilation is outward need to invert halves */
        left = epochdatas[:len(epochdatas)//2][::-1]
        right = epochdatas[len(epochdatas)//2:][::-1]
        epochdatas = left + right
    /* Now that all data has been seen, start the attack */
    /* Flag for oscilation attack */
    osc = False
    while len(epochdatas) > 0 do
        /* Pretend reading data and throw it away */
        b' = getbatch()
        if BTCH == "batch" then
            | batchsize = 1
        else
            | batchsize = len(b')
        /* Batching data from low to high */
        if ATK == "lowhigh" then
            | batch b = epochdata[:batchsize]
            | epochdata = epochdata[batchsize:]
        /* Batching data from high to low */
        if ATK == "highlow" then
            | batch b = epochdata[-batchsize:]
            | epochdata = epochdata[:-batchsize]
        /* Batching data with oscillating losses */
        if ATK == "oscillating in" or "oscillating out" then
            osc = not osc
            if osc then
                | batch b = epochdata[-batchsize:]
                | epochdata = epochdata[:-batchsize]
            else
                | batch b = epochdata[:batchsize]
                | epochdata = epochdata[batchsize:]
        train(M,  $\mathcal{L}_M$ , b)
        train(S,  $\mathcal{L}_S$ , b)

```

precise, this term can be explicitly manipulated to produce a better attack against SGD convergence. In particular, from the expression above, the attacker needs to pick out batches such that the difference between the batch gradient and the true gradient is in the opposite direction from the true gradient. In this paper, instead of the gradient of the loss, we approximate this information by using the loss error term directly, which is much less expensive and can be utilized in practice.

In particular, we observe that the optimisation does not converge even for a simple two-variable linear regression as is shown in Appendix C.

B Upper bound on sample size for poisoning attacks

In this section we further investigate an attacker’s ability to approximate out-of-distribution data using natural data. In the limit of large batch size, we expect the gradients of the input to be normally distributed due to the central limit theorem. As a result, we expect to be able to approximate any vector in the limit of infinite batches, as long as we sample for long enough. To make this statement more concrete, we compute an upper bound on the sample size for a fixed $(1 - p)$ -confidence interval of size 2ϵ as follows. Using the notation from the section above, denote individual item losses $L_j(\theta_k)$ such that $\hat{L}_{i_k}(\theta_k) = \frac{1}{B} \sum_{j=i_k}^{i_k+B} L_j(\theta_k)$, where B is the batch size. The attacker aims to pick $j \sim J$, such that we can match the target gradient with a natural one:

$$\nabla L^\dagger(\theta_k) = \frac{1}{B} \sum_{j=1}^B \nabla L_j(\theta_k). \quad (18)$$

As stated previously, we will assume in our calculations that batch size is large enough for us to approximate the right hand side of Equation (18) using the central limit theorem, reducing our problem to finding an optimal sample $y \sim \mathcal{N}(\mu, \sigma^2)$ such that:

$$\|\nabla L^\dagger(\theta_k) - y\| \leq \epsilon \quad (19)$$

Let $Z \sim \mathcal{N}(0, 1)$, with CDF Φ and PDF ϕ . Let Y_1, \dots, Y_n be iid $\mathcal{N}(\mu, \sigma)$. Let $K_i = \|\nabla L^\dagger - Y_i\|$ have CDF Φ' . We want $K^{(1)} = \min K_i$ to be within ϵ of the desired value with probability $1 - p$:

$$\mathbb{P}(K^{(1)} \leq \epsilon) = 1 - p \iff \quad (20)$$

$$1 - (1 - \Phi'(\epsilon))^n = 1 - p \iff \quad (21)$$

$$\ln p = n \ln(1 - \Phi'(\epsilon)) \iff \quad (22)$$

$$n = \frac{\ln p}{\ln(1 - \Phi'(\epsilon))} \quad (23)$$

Now, in the case of 1D and l_1 -norm, $\Phi'(\epsilon) = \Phi(\frac{\epsilon - \mu + \nabla L^\dagger}{\sigma}) - \Phi(\frac{-\epsilon - \mu + \nabla L^\dagger}{\sigma})$. Hence our equation for n is:

$$n = \frac{\ln p}{\ln \left[1 - \Phi\left(\frac{\epsilon - \mu + \nabla L^\dagger}{\sigma}\right) + \Phi\left(\frac{-\epsilon - \mu + \nabla L^\dagger}{\sigma}\right) \right]} \quad (24)$$

In fact for small values of $\frac{\epsilon}{\sigma}$, we can expand to first order and approximate as:

$$n = \frac{\ln p}{\ln \left[1 - 2\frac{\epsilon}{\sigma} \phi\left(\frac{-\mu + \nabla L^\dagger}{\sigma}\right) \right]} \quad (25)$$

where we can approximate true parameters through $\mu = \frac{1}{N} \sum_i \hat{L}_i(\theta_k)$, $\sigma = \frac{1}{B(N-1)} \sum_i (\hat{L}_i(\theta_k) - \mu)^2$. In the general case, we are dealing with multidimensional gradients. However we can once again invoke CLT to approximate the RHS with a multivariate normal distribution $y \sim \mathcal{N}(\mu, \Sigma)$. Given this reformulated problem, we can see that in the general case, the reconstruction is impossible – as the covariance matrix must be non-singular. This can be seen from the following simple example. Say we are trying to approximate $y = \begin{bmatrix} 1 \\ 1 \end{bmatrix}$ using samples from the distribution $\begin{bmatrix} X \\ 2X \end{bmatrix}$ where X is a Gaussian random variable. Clearly we can not get within **any** accuracy with this reconstruction. In fact the closest one can get is within 0.5 at $x = 0.5$. Therefore, we will assume that we have a non-singular covariance matrix. Write $Y = AZ + \mu$, where $\Sigma = AA^T$ and Z is a vector of independent gaussians. One can now attain exact

bounds using *e.g.* non central chi-squared distribution, though for us a rough bound would be enough. For this, note $K_i = \|\nabla L^\dagger - \mathbf{Y}_i\| \leq \|A^{-1}(\nabla L^\dagger - \boldsymbol{\mu}) - \mathbf{Z}_i\| \|A\|$. Therefore, we can see that the following n is sufficient:

$$n = \max_i \frac{\ln 1 - [1 - p]^{\frac{1}{k}}}{\ln [1 - \Phi(\frac{\epsilon}{\|A\|} + [A^{-1}(\nabla L^\dagger - \boldsymbol{\mu})]_i) + \Phi(\frac{-\epsilon}{\|A\|} + [A^{-1}(\nabla L^\dagger - \boldsymbol{\mu})]_i)]} \quad (26)$$

Or similarly approximating for small values of $\frac{\epsilon}{\|A\|}$:

$$n = \max_i \frac{\ln 1 - [1 - p]^{\frac{1}{k}}}{\ln [1 - \frac{2\epsilon}{\|A\|} \phi([A^{-1}(\nabla L^\dagger - \boldsymbol{\mu})]_i)]} \quad (27)$$

C Stochastic gradient descent with linear regression

In this section we investigate the impact of ordered data on stochastic gradient descent learning of a linear regression model. The problem in this case is optimising a function of two parameters:

$$J(\theta_0, \theta_1) = \frac{1}{n} \sum_{i=1}^n \|\beta_\theta(x_i) - y_i\|^2$$

$$\beta_\theta(x) = \theta_1 x + \theta_0$$

By considering data points coming from $y = 2x + 17 + \mathcal{N}(0, 1)$, we attempt to approximate the values of θ_0, θ_1 . We observe that even in such a simple 2-parameter example, we are able to disrupt convergence by reordering items that the model sees during gradient descent. This shows that the inherent ‘vulnerability’ lies in the optimization process itself, rather than in overparametrized learned models. The following two subsections investigate this problem in three different choices of batch size and learning rate.

C.1 Batch reshuffling

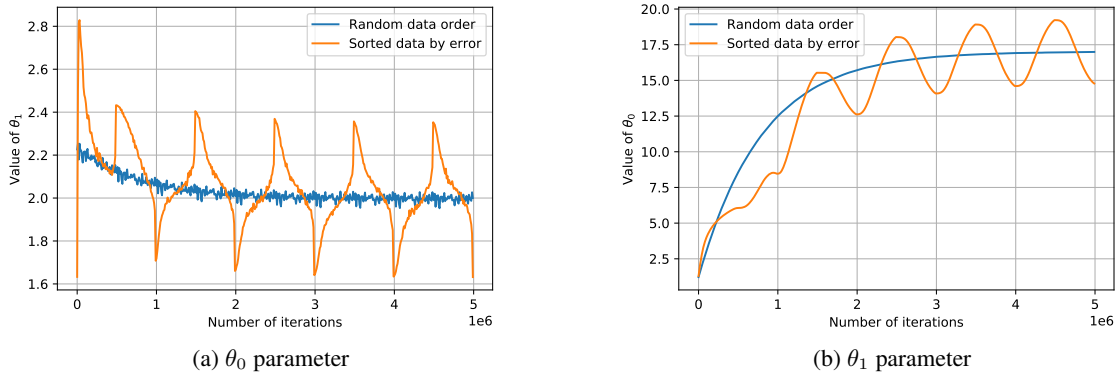


Figure 9: Individual linear regression parameters changing over the course the training

Figure 10 shows average error per data point, when training is done over randomly-sampled data and ordered by error data. A linear regression here has an optimal solution that the blue line reaches while the orange line oscillates quite far away from it. In fact, by looking at the parameter behaviour, as shown on Figure 9, we can see that the parameters end up oscillating around the global minimum, never reaching it. Indeed, we find that with error-ordered data, gradient descent exhibits strong overfitting to the data samples in the current minibatch, and fails to reach the optimal solution. This effect is similar to the one observed for SGD with neural networks. In addition, we can also see the dependence of the oscillations on the learning rate. On Figure 11 by increasing the step size by 10 times from $5e^{-6}$ to $5e^{-5}$, we are able to drastically increase oscillations for θ_0 . This behaviour is achieved when our minibatch size is chosen to be equal to 1.

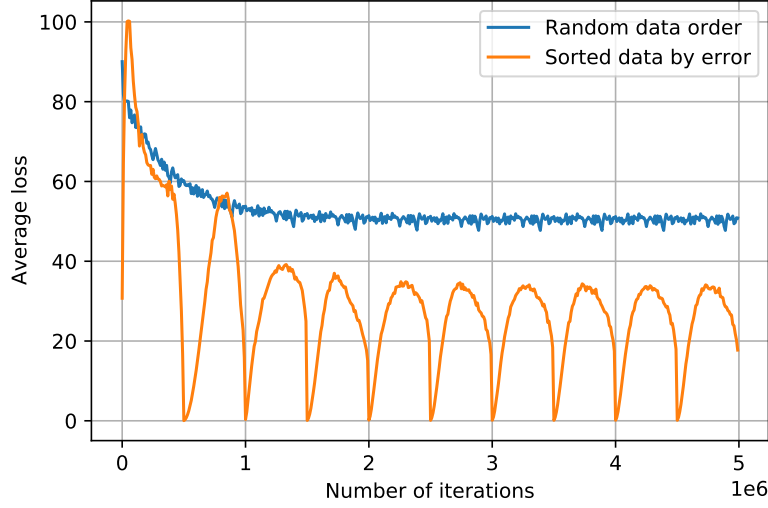


Figure 10: Average training dataset loss during stochastic gradient descent of a linear regression model with two parameters. Random sampling is shown in blue, sorted items by error are shown in yellow.

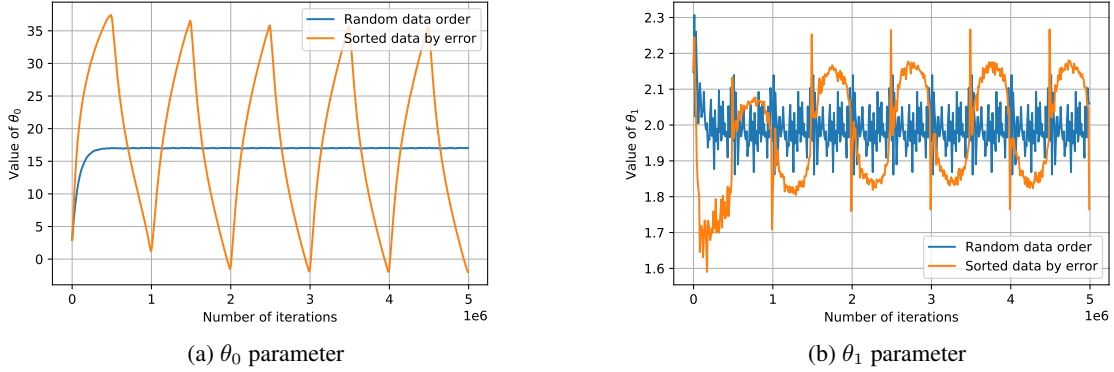


Figure 11: Individual linear regression parameters changing over the course the training for larger step size

C.2 Batch reordering

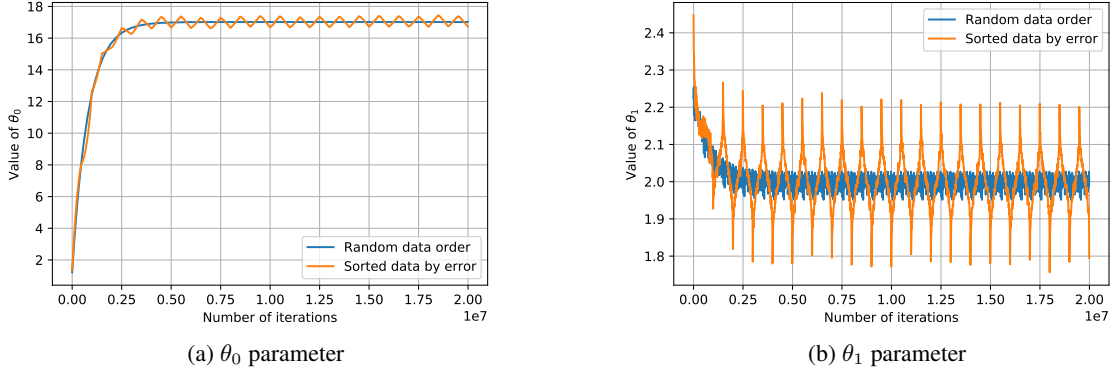
By increasing the minibatch size, we are able to 'dampen' the oscillations observed in the previous subsection and converge to the optimal solution, as shown on Figure 12. This is also quite similar to the neural network case, as simple batch reordering is not able to achieve the same performance degradation as reshuffling.

D Batch reshuffling and hyperparameters

We have thoroughly evaluated different combinations of hyperparameters for the integrity attack (Table 4) and show the results in Figures 13 to 24.

E Whitebox batching attack performance

We show training of ResNet18 with the CIFAR10 dataset in the presence of whitebox BRRR attacks in Figure 25. We see that datapoint-wise attacks perform extremely well, while batchwise BRRR attacks force the network to memorise the training data and reduce its testing data performance.

Figure 12: Individual linear regression parameters changing over the course the training for larger batch size ($B=4$)

Parameter	Values
Source model	ResNet18
Surrogate model	LeNet-5
Dataset	CIFAR10
Attack policies	[HighLow, LowHigh, Oscillations in, Oscillations out]
Batch sizes	[32, 64, 128]
True model optimizers	[Adam, SGD]
Surrogate model optimizers	[Adam, SGD]
Learning rates	[0.1, 0.01, 0.001]
Surrogate learning rates	[0.1, 0.01, 0.001]
Moments	[0, 0.5, 0.99]
Surrogate moments	[0, 0.5, 0.99]

Table 4: Parameters searched

F Triggered training

Training of models with BOB are shown in Figures 26 to 29. We show training, test, trigger accuracies, and overall mistakes introduced by the trigger. The target network is VGG16 and the surrogate is ResNet-18.

Here, the attacker uses up to 20 BOB batches every 50000 natural datapoints for 10 epochs and then uses 90 pure BOB batches. Individual lines refer to training of different models with various parameter initialisation and trigger target classes. Note that the non-BOB baseline here gets zero trigger accuracy.

Overall, BOB controls the performance of the model extremely well in a whitebox setup, while performance decreases in the blackbox case. There is clear difference in trigger performance between different target classes, yet the attack works across them without disrupting the overall model generalisation.

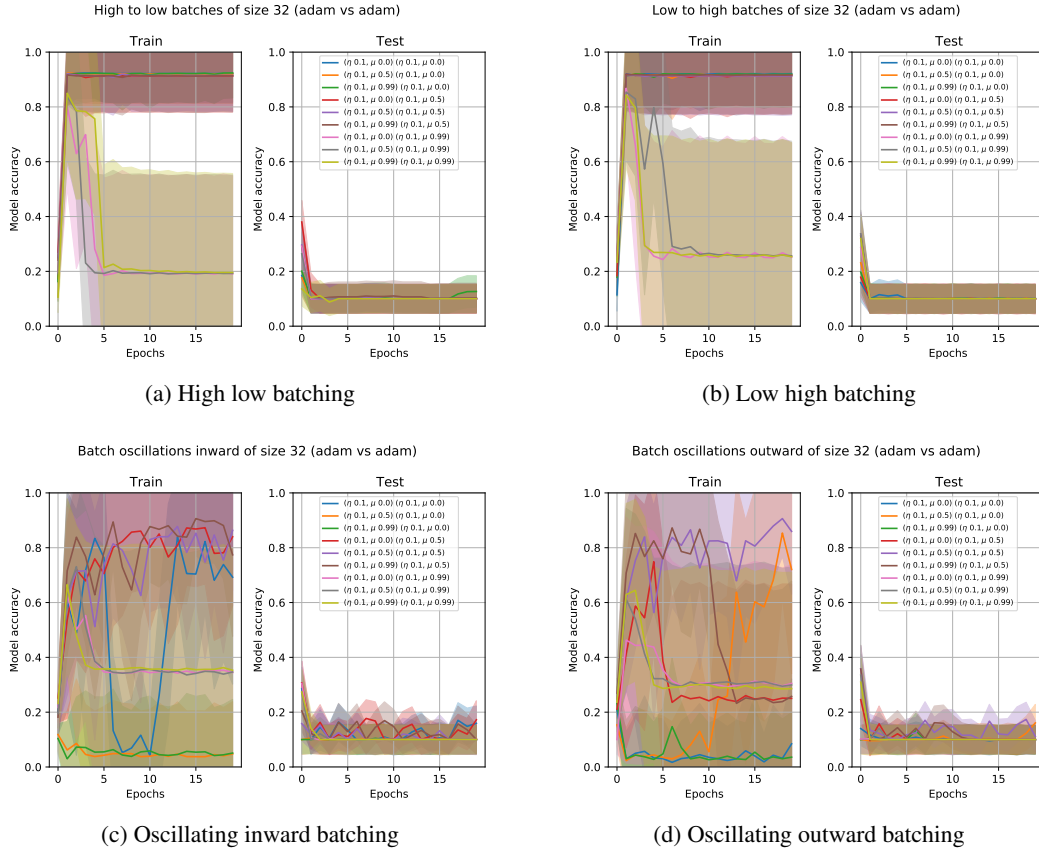


Figure 13: ResNet18 real model Adam training, LeNet5 surrogate with Adam and Batchsize 32

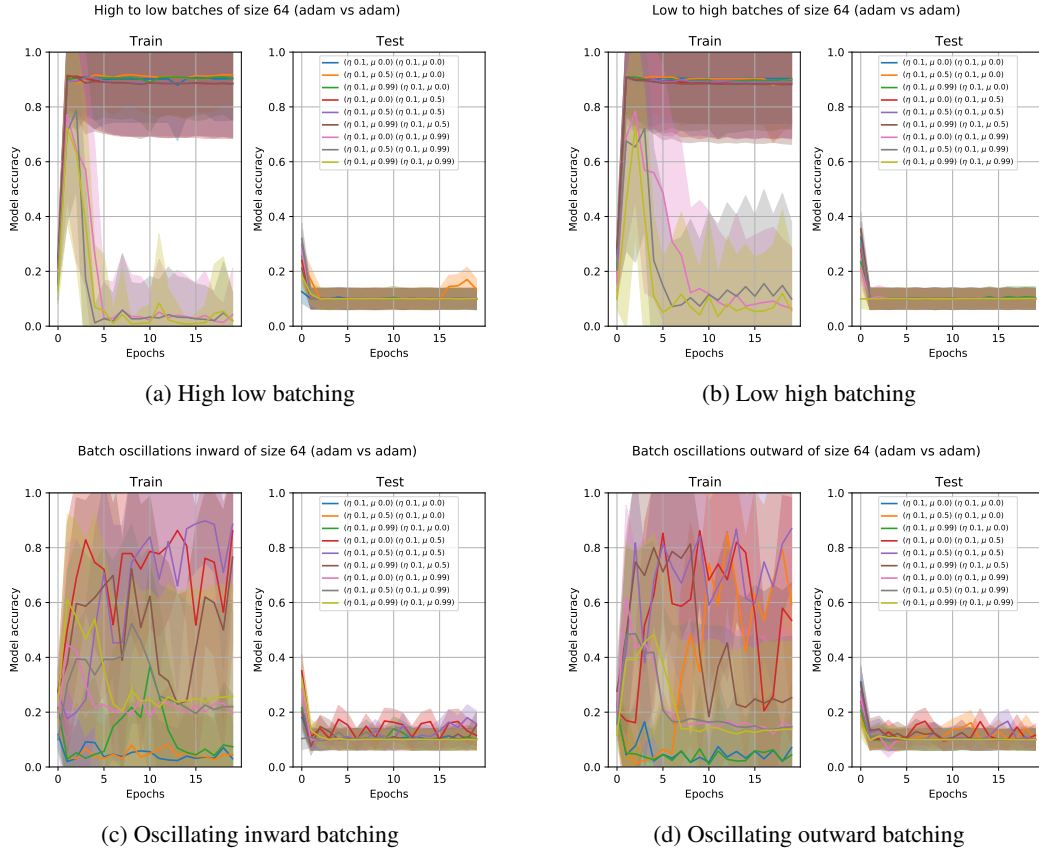


Figure 14: ResNet18 real model Adam training, LeNet5 surrogate with Adam and Batchsize 64

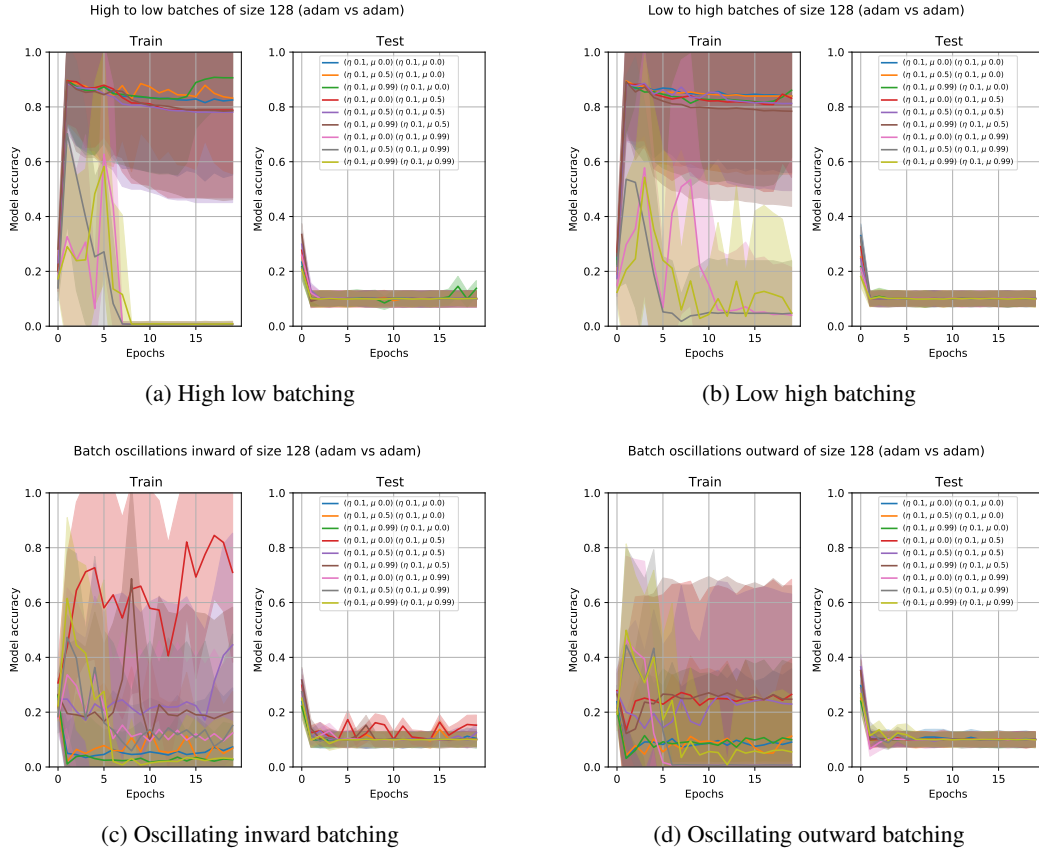


Figure 15: ResNet18 real model Adam training, LeNet5 surrogate with Adam and Batchsize 128

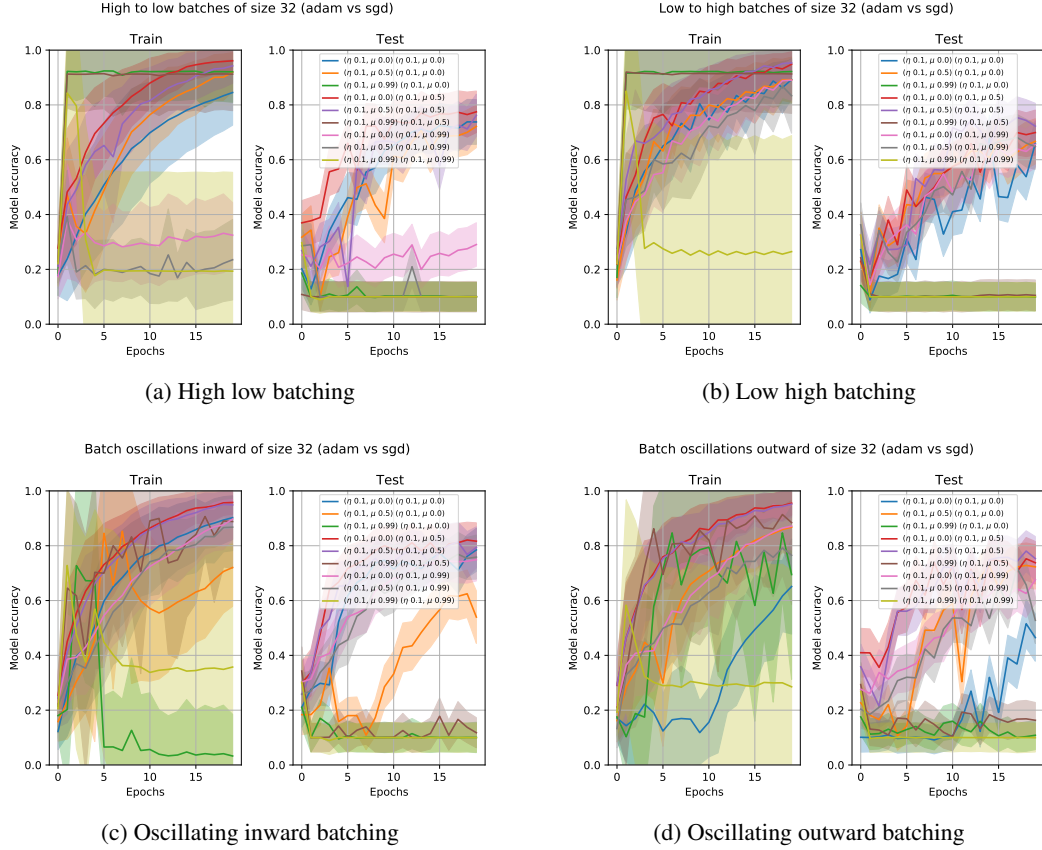


Figure 16: ResNet18 real model Adam training, LeNet5 surrogate with SGD and Batchsize 32

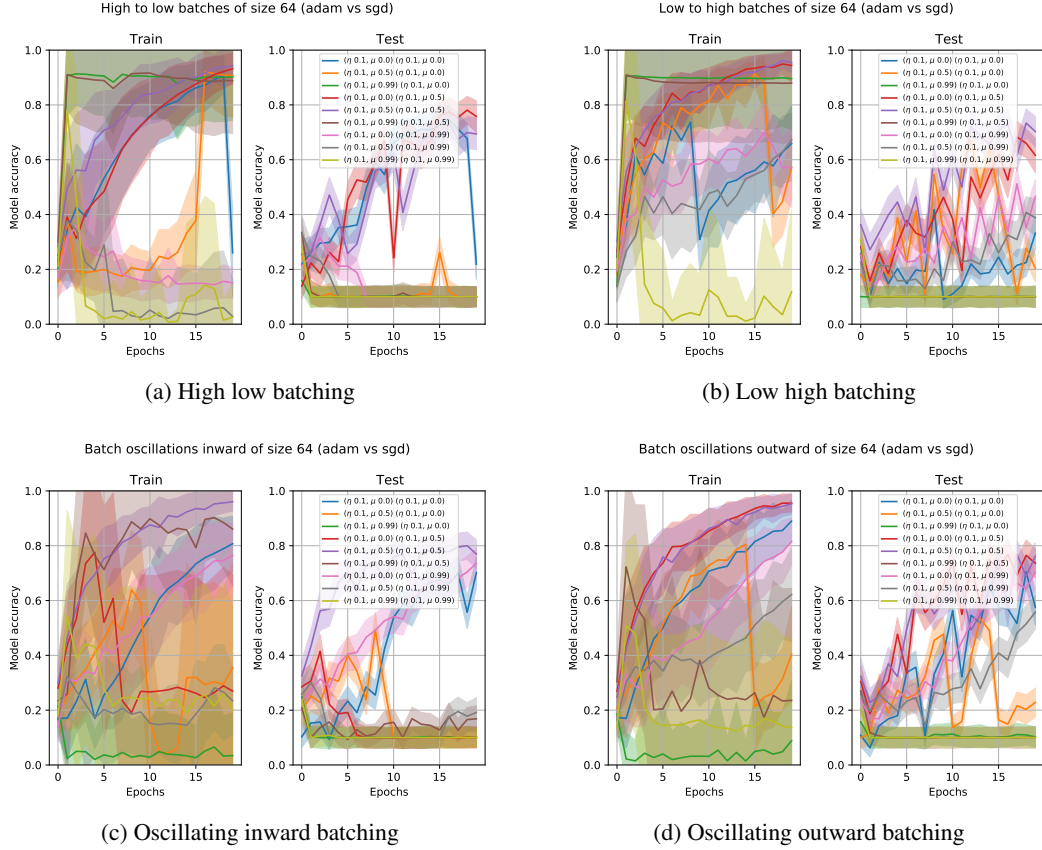


Figure 17: ResNet18 real model Adam training, LeNet5 surrogate with SGD and Batchsize 64

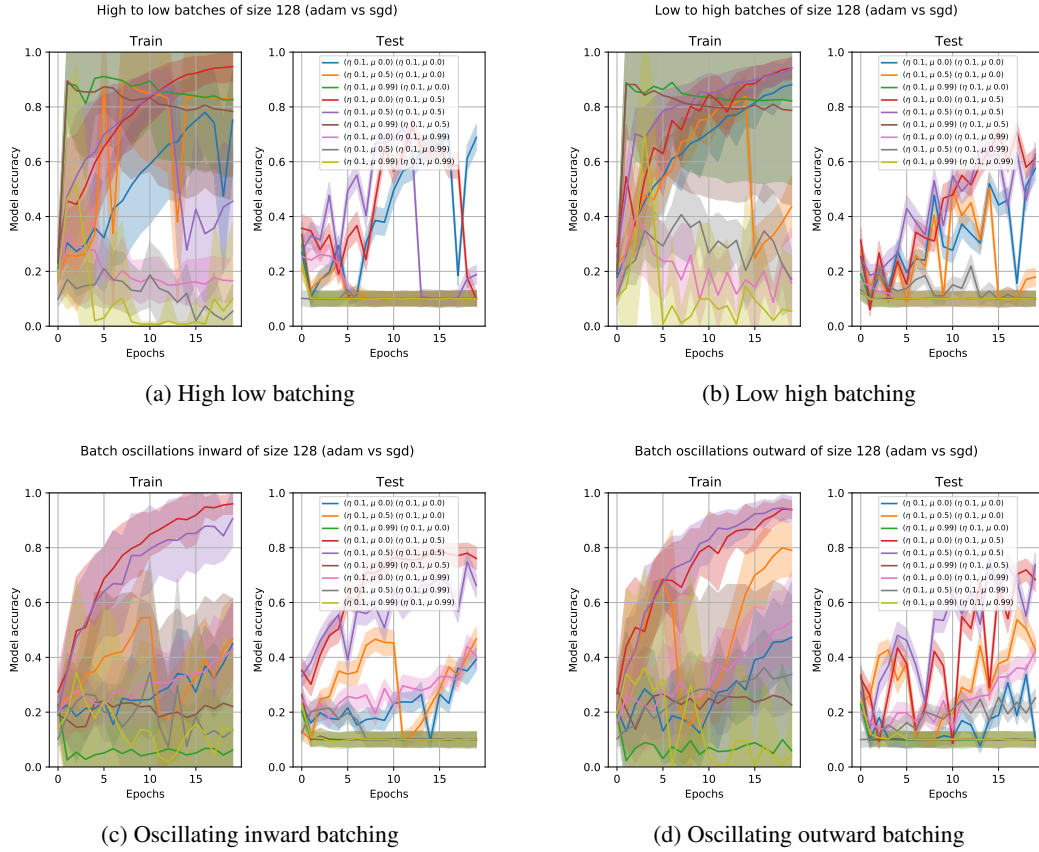


Figure 18: ResNet18 real model Adam training, LeNet5 surrogate with SGD and Batchsize 128

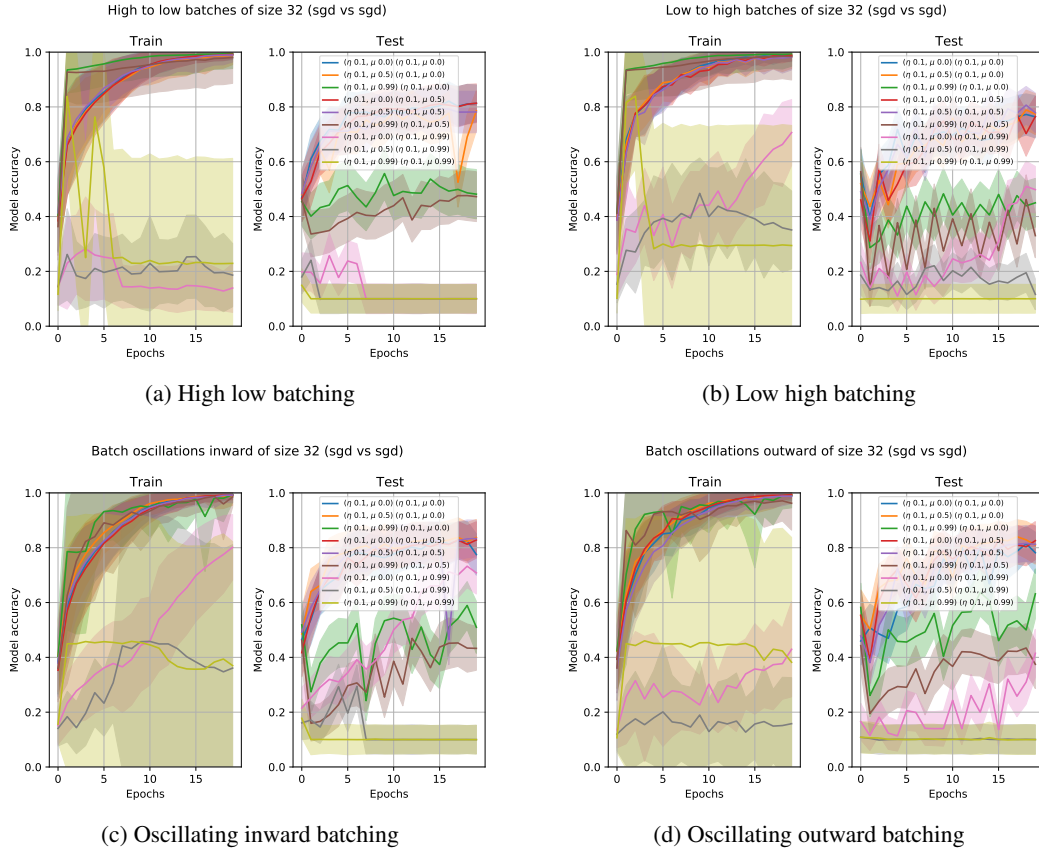


Figure 19: ResNet18 real model SGD training, LeNet5 surrogate with SGD and Batchsize 32

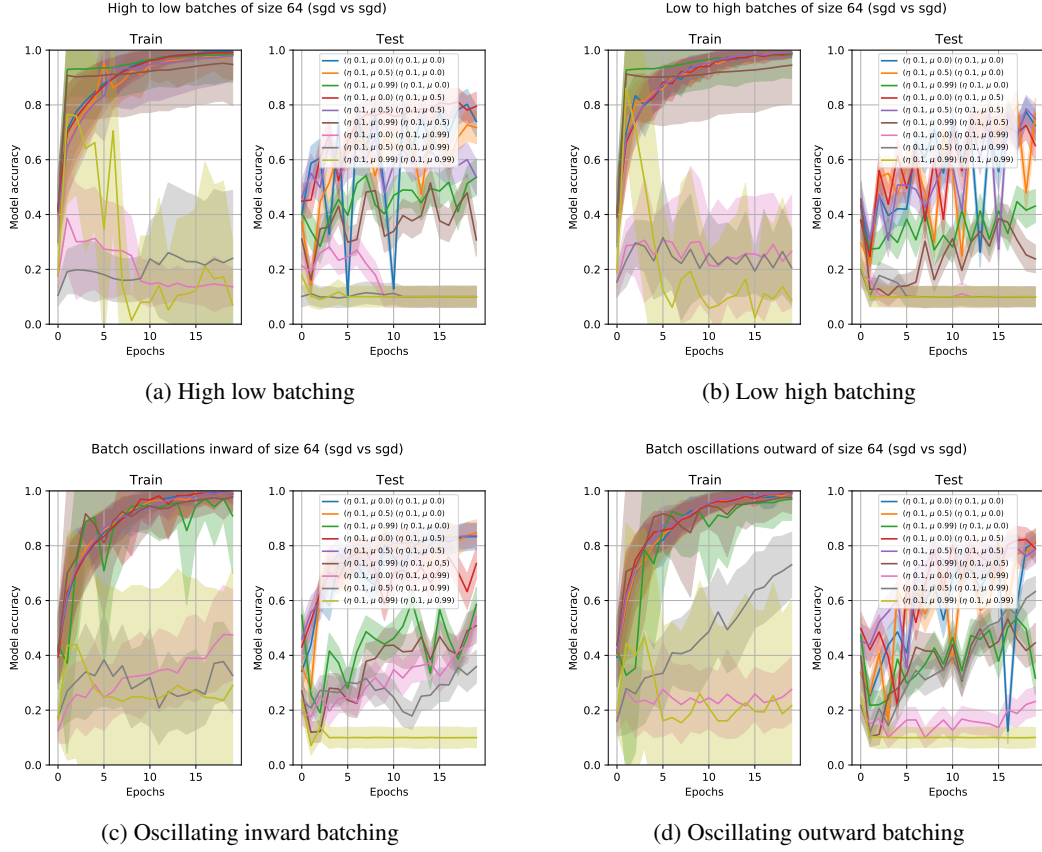


Figure 20: ResNet18 real model SGD training, LeNet5 surrogate with SGD and Batchsize 64

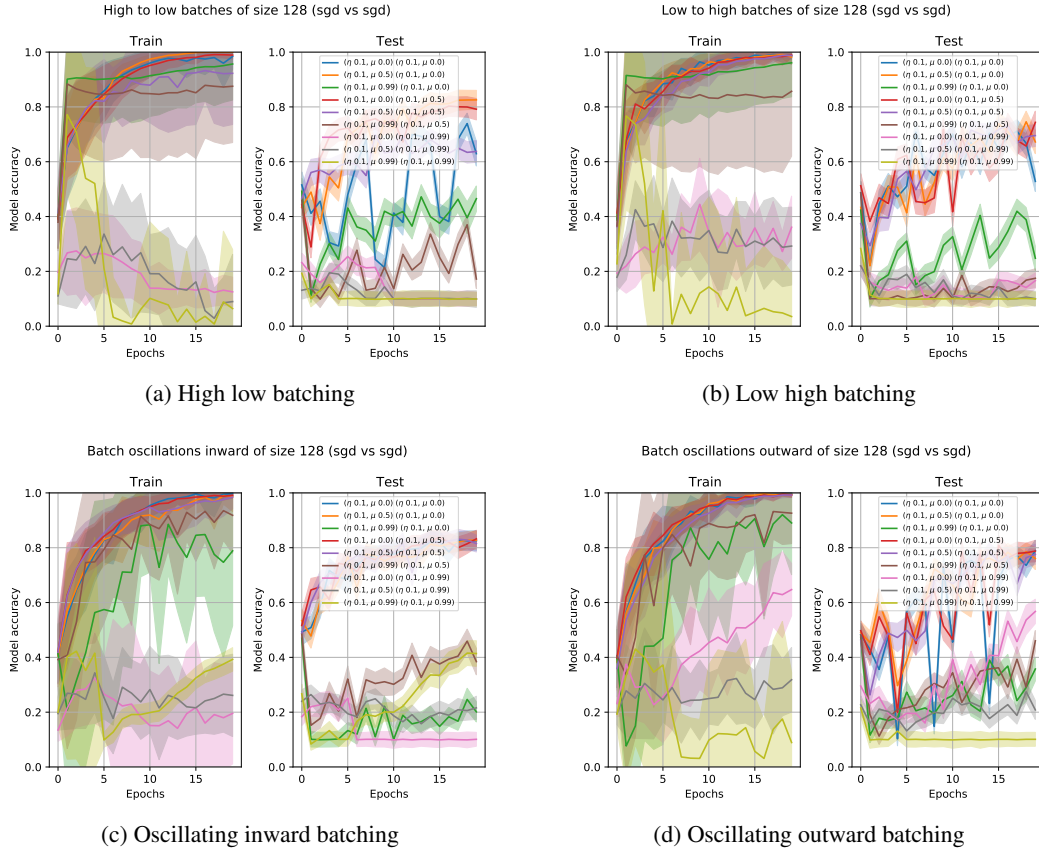


Figure 21: ResNet18 real model SGD training, LeNet5 surrogate with SGD and Batchsize 128

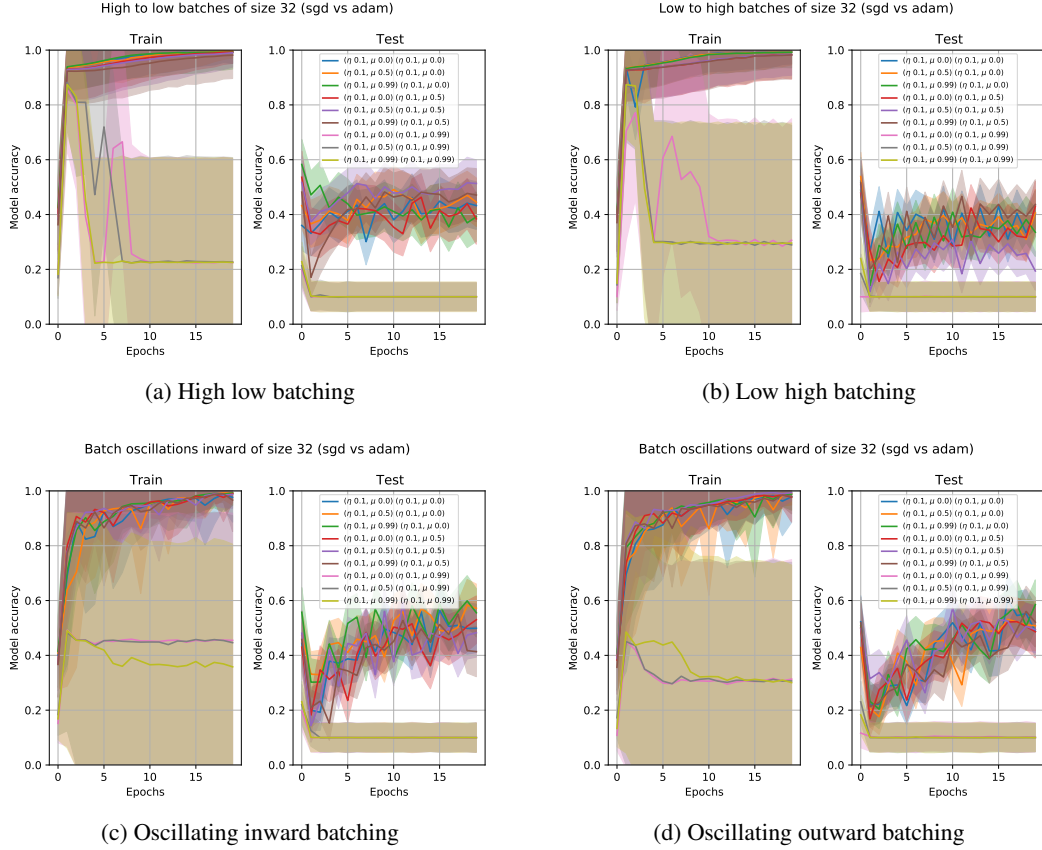


Figure 22: ResNet18 real model SGD training, LeNet5 surrogate with Adam and Batchsize 32

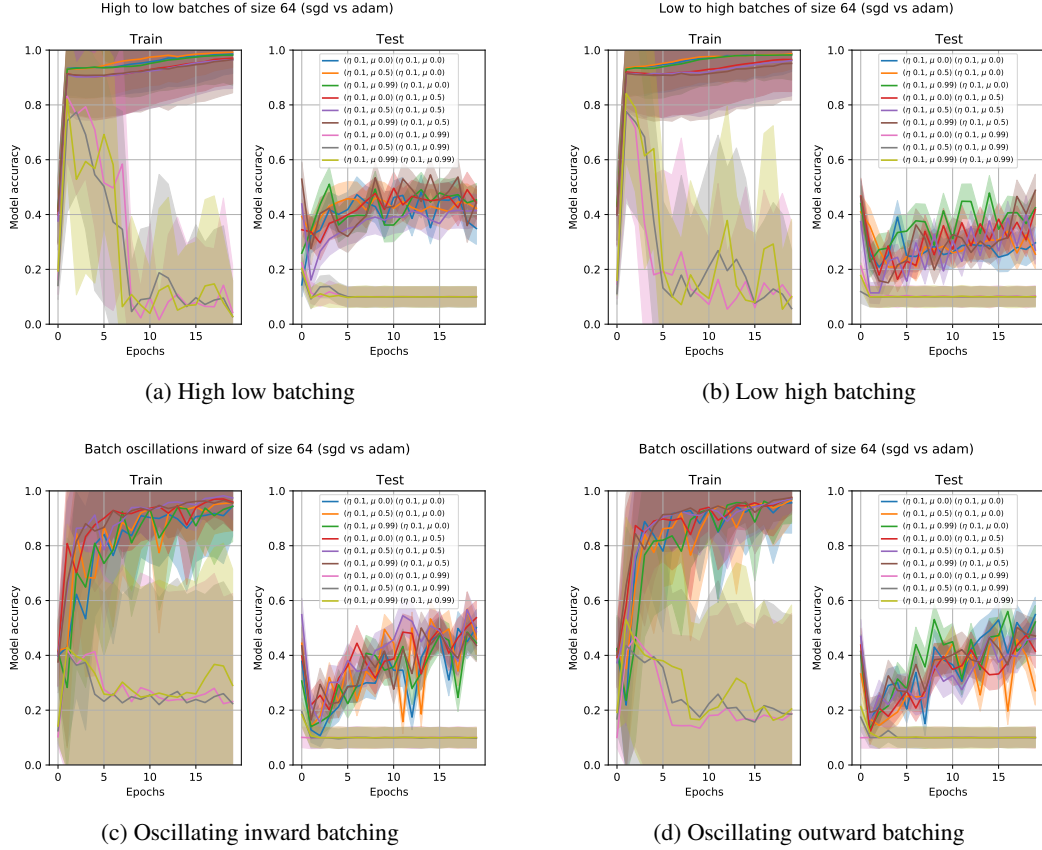


Figure 23: ResNet18 real model SGD training, LeNet5 surrogate with Adam and Batchsize 64

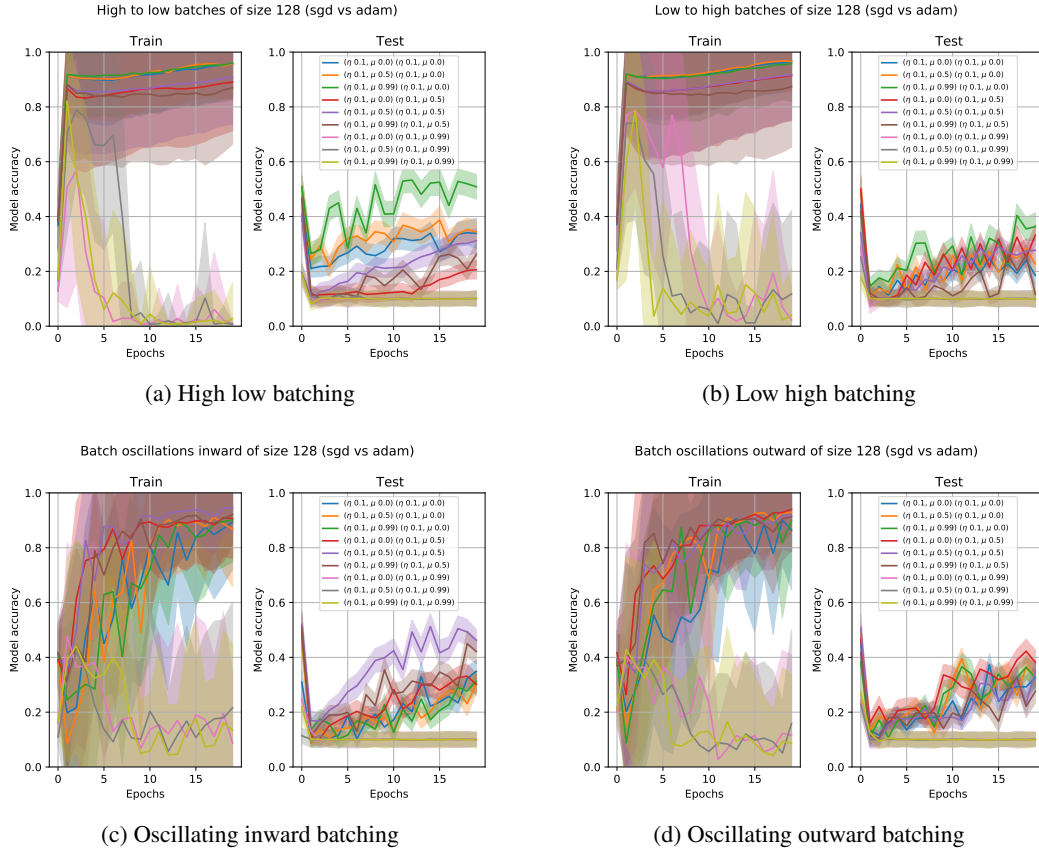


Figure 24: ResNet18 real model SGD training, LeNet5 surrogate with Adam and Batchsize 128

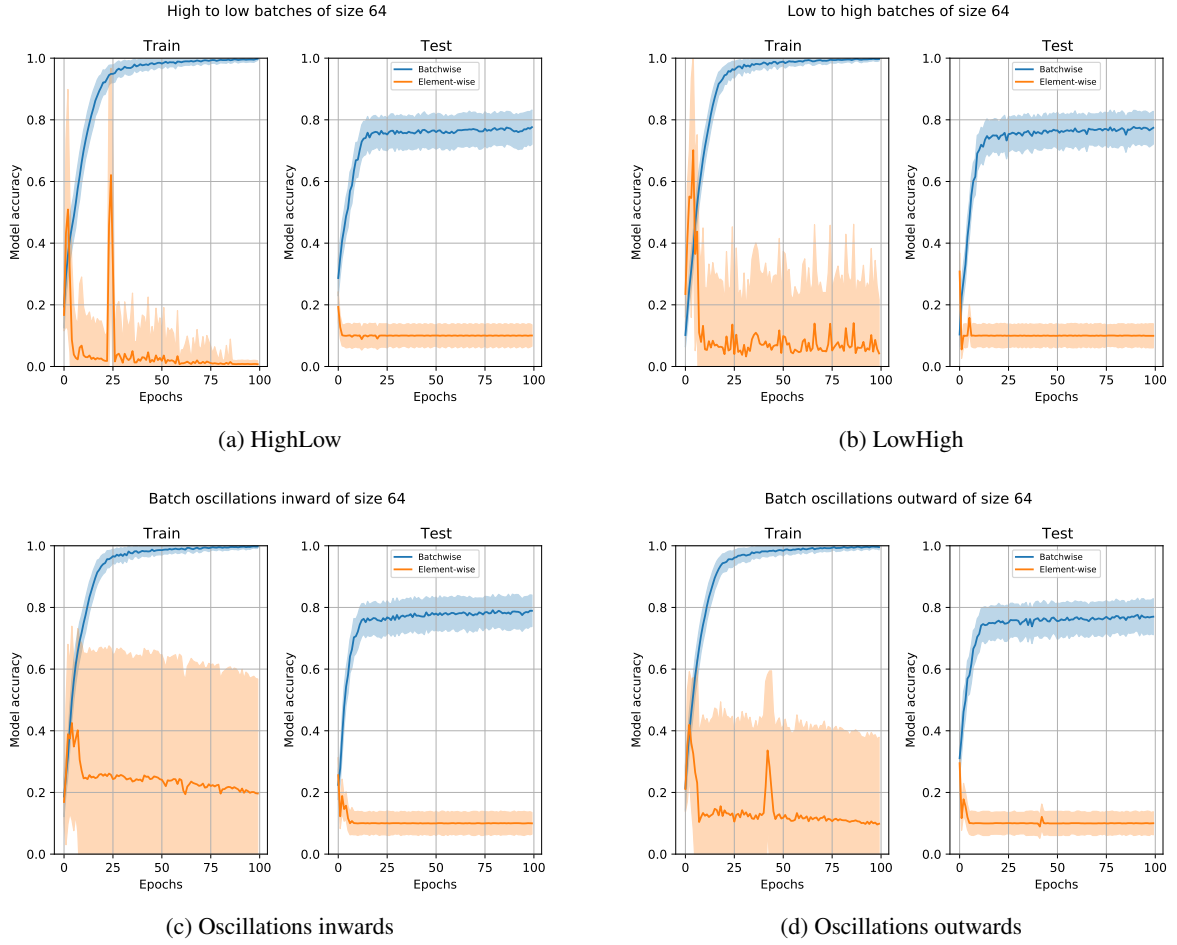


Figure 25: Whitebox performance of the Batching attacks – CIFAR10.



(a) 32 batchsize



(b) 64 batchsize



(c) 128 batchsize

Figure 26: Trigger ordered training with blackbox 9 whitelines trigger.



(a) 32 batchsize

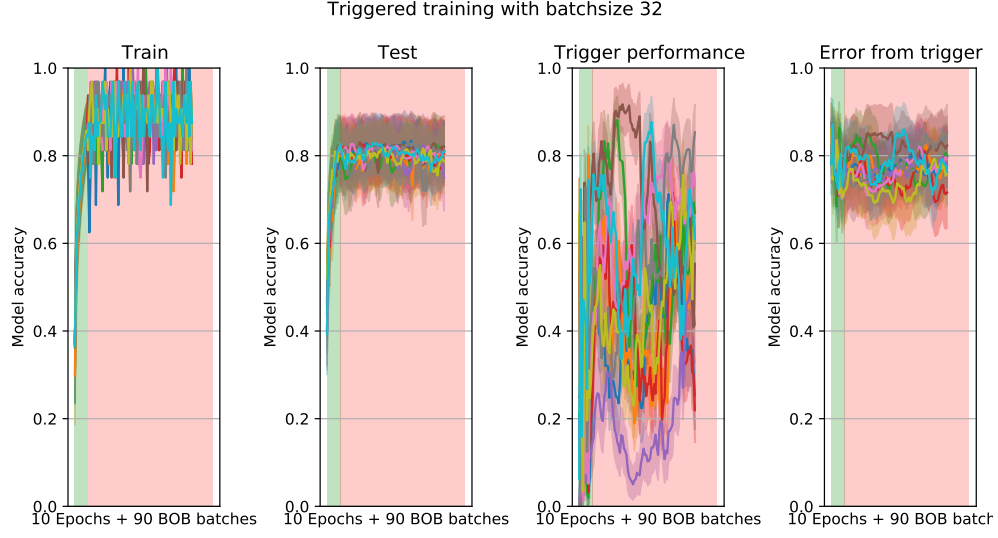


(b) 64 batchsize

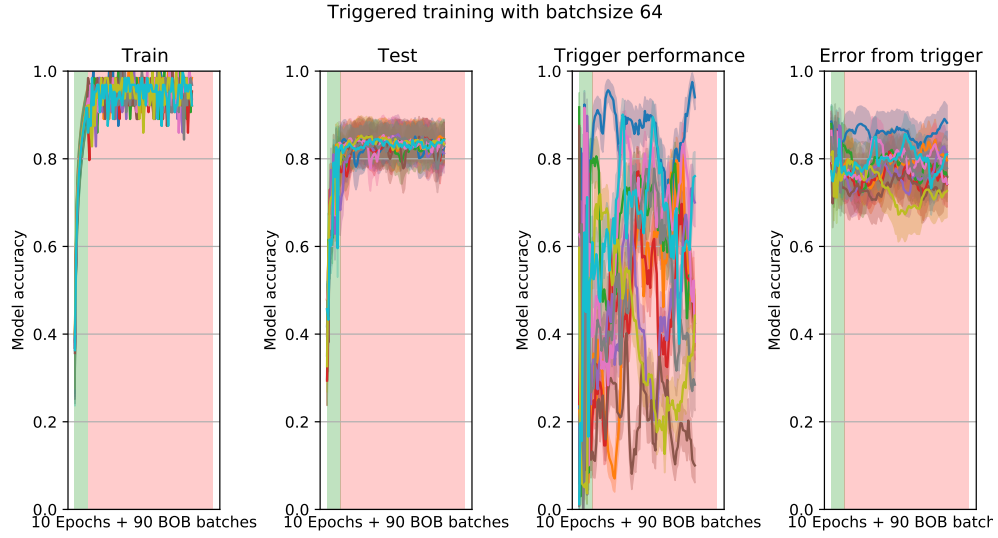


(c) 128 batchsize

Figure 27: Trigger ordered training with whitebox 9 whitelines trigger.



(a) 32 batchsize



(b) 64 batchsize



(c) 128 batchsize

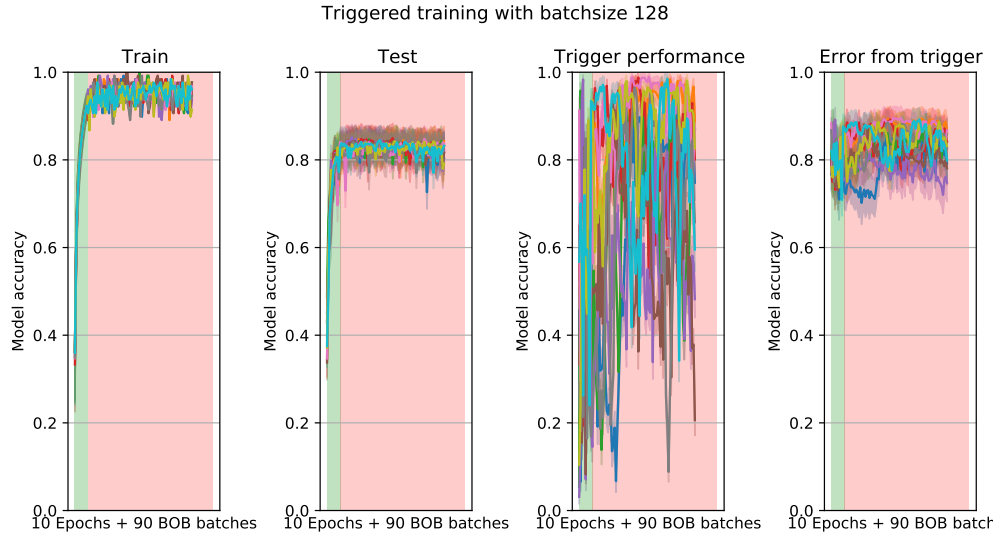
Figure 28: Trigger ordered training with blackbox flaglike trigger.



(a) 32 batchsize



(b) 64 batchsize



(c) 128 batchsize

Figure 29: Trigger ordered training with whitebox flaglike trigger.